PROTOCOL REPORT

Demonstration of Helicopter Multi-Towed Array Detection System (MTADS) Magnetometry Technology at Pueblo Precision Bombing Range #2, Colorado

ESTCP Project MM-0535

AUGUST 2008

Sky Research, Inc.

Environmental Security Technology Certification Program

Report Documentation Page

Form Approved
OMB No. 0704-0188

1. REPORT DATE	2. REPORT TYPE	3. DATES COVERED
01 AUG 2008	**N/A**	**-**

4. TITLE AND SUBTITLE	5a. CONTRACT NUMBER
Demonstration of Helicopter Multi-Towed Array Detection System (MTADS) Magnetometry Technology at Pueblo Precision Bombing Range #2, Colorado - PROTOCOL REPORT	5b. GRANT NUMBER
	5c. PROGRAM ELEMENT NUMBER
6. AUTHOR(S)	5d. PROJECT NUMBER
	5e. TASK NUMBER
	5f. WORK UNIT NUMBER
7. PERFORMING ORGANIZATION NAME(S) AND ADDRESS(ES) **Sky Research, Inc.**	8. PERFORMING ORGANIZATION REPORT NUMBER
9. SPONSORING/MONITORING AGENCY NAME(S) AND ADDRESS(ES)	10. SPONSOR/MONITOR'S ACRONYM(S)
	11. SPONSOR/MONITOR'S REPORT NUMBER(S)

12. DISTRIBUTION/AVAILABILITY STATEMENT
Approved for public release, distribution unlimited

13. SUPPLEMENTARY NOTES
The original document contains color images.

14. ABSTRACT

15. SUBJECT TERMS

16. SECURITY CLASSIFICATION OF:			17. LIMITATION OF ABSTRACT	18. NUMBER OF PAGES	19a. NAME OF RESPONSIBLE PERSON
a. REPORT	b. ABSTRACT	c. THIS PAGE			
unclassified	**unclassified**	**unclassified**	**UU**	**58**	

Standard Form 298 (Rev. 8-98)
Prescribed by ANSI Std Z39-18

Environmental Security Technology Certification Program (ESTCP)

Final Report

Demonstration of Helicopter Multi-Towed Array Detection System (MTADS) Magnetometry Technology at Pueblo Precision Bombing Range #2, Colorado

Project No. 200535: Innovative Multi-Sensor Airborne Wide Area Assessment of UXO Sites

August 28, 2008
Version 2.0

REPORT DOCUMENTATION PAGE

Form Approved
OMB No. 0704-0188

PLEASE DO NOT RETURN YOUR FORM TO THE ABOVE ORGANIZATION.

1. REPORT DATE *(DD-MM-YYYY)*	2. REPORT TYPE	3. DATES COVERED *(From - To)*
08-28-2008	Final, V2	May 2005 - August 2008

4. TITLE AND SUBTITLE

Demonstration of Helicopter Multi-Towed Array Detection System (MTADS) Magnetometry Technology at Pueblo Precision Bombing Range #2, Colorado

5a. CONTRACT NUMBER

W912HQ-05-C-0036

5b. GRANT NUMBER

5c. PROGRAM ELEMENT NUMBER

MM-0535

6. AUTHOR(S)

Dr. Jack Foley
Mr. David Wright

5d. PROJECT NUMBER

5e. TASK NUMBER

5f. WORK UNIT NUMBER

7. PERFORMING ORGANIZATION NAME(S) AND ADDRESS(ES)

Sky Research, Inc.
445 Dead Indian Memorial Rd.
Ashland, OR 97520

8. PERFORMING ORGANIZATION REPORT NUMBER

9. SPONSORING/MONITORING AGENCY NAME(S) AND ADDRESS(ES)

Environmental Security Technology Certification Program Office
901 North Stuart Street, Suite 303
Arlington, VA 22203-1821

10. SPONSOR/MONITOR'S ACRONYM(S)

ESTCP

11. SPONSOR/MONITOR'S REPORT NUMBER(S)

12. DISTRIBUTION/AVAILABILITY STATEMENT

Unlimited

13. SUPPLEMENTARY NOTES

14. ABSTRACT

The Pueblo Precision Bombing Range is located in Otero County, Colorado. This site is classified by the United States Government as a Formerly Used Defense Site (FUDS) and was a World War II-era military training facility. This demonstration utilized Helicopter Multi-sensor Towed Array Detection System (MTADS) Magnetometry (HeliMag) technology, a wide area assessment technology. A data collection survey was conducted in September of 2005 and resulted in the survey of over 5,000 acres. Targets were selected using automatic picking procedures and 12,735 anomalies were selected from the data to assess the distribution of metal objects across the study area. A subset of anomalies in each of the areas of interest were analyzed using dipole fit analysis, the results of which were used to down-select candidate targets for intrusive investigation. These intrusive investigation results were used for verification of HeliMag results.

15. SUBJECT TERMS

Helicopter magnetometry, airborne magnetometry, HeiMag, wide area assessment, Pueblo Precision Bombing Range #2

16. SECURITY CLASSIFICATION OF:			17. LIMITATION OF ABSTRACT	18. NUMBER OF PAGES	19a. NAME OF RESPONSIBLE PERSON
a. REPORT	b. ABSTRACT	c. THIS PAGE		57	Dr. John Foley
					19b. TELEPHONE NUMBER *(Include area code)* 541.552.5141

Reset

Standard Form 298 (Rev. 8/98)
Prescribed by ANSI Std. Z39.18

TABLE OF CONTENTS

LIST OF FIGURES

LIST OF TABLES

ACRONYMS

AAF	Army Air Force
AGL	Above Ground Level
ASR	Archive Search Report
BT3	Bomb Target 3
BT4	Bomb Target 4
CRADA	Cooperative Research and Development Agreement
cm	centimeter(s)
Cs	Cesium
CSM	Conceptual Site Model
DAQ	Data Acquisition Computer
DERP	Defense Environmental Restoration Program
DGM	Digital Geophysical Mapping
DoD	Department of Defense
DSB	Defense Science Board
ESTCP	Environmental Security Technology Certification Program
FUDS	Formerly Used Defense Sites
GIS	Geographic Information Systems
GPS	Global Positioning System
HE	High Explosive
HeliMag	Helicopter MTADS Magnetometry (see MTADS)
HSI	Hyperspectral imaging
Hz	hertz
IMU	Inertial Measurement Unit
lb	pound
LiDAR	Light Detection and Ranging
m	meter(s)
m/s	meters per second
MEC	Munitions and Explosives of Concern
MTADS	Multi-Sensor Towed Array Detection System
NE	northeast
NRL	Naval Research Laboratory
nT	nanotesla
OB/OD	Open Burn/Open Detonation
PBR	Precision Bombing Range
PPS	Pulse Per Second
RTK GPS	Real-Time Kinematic Global Positioning System
SAR	Synthetic Aperture Radar
SW	southwest
TOA	Time of Applicability
UTC	Coordinated Universal Time
UTM	Universal Transverse Mercator
UXO	Unexploded Ordnance
WAA	Wide Area Assessment

ACKNOWLEDGMENTS

Demonstration of Helicopter Multi-Towed Array Detection System (MTADS) Magnetometry at Pueblo Precision Bombing Range #2, Colorado documents the acquisition, processing, analysis, and interpretation of Helicopter Multi-Towed Array Detection System Magnetometry data for unexploded ordnance related sites at the former Pueblo Precision Bombing Range #2. The work was performed by Sky Research, Inc. of Oregon, with Dr. John Foley serving as Principal Investigator, and Mr. David Wright, formerly of AETC and now with Sky Research serving as co-Principal Investigator.

Funding for this project was provided by the Environmental Security Technology Certification Program Office. This project offered the opportunity to examine advanced airborne methods as part of the Department of Defense's efforts to evaluate wide area assessment technologies for efficient the characterization and investigation of large Department of Defense sites.

We wish to express our sincere appreciation to Dr. Jeffrey Marqusee, Dr. Anne Andrews, and Ms. Katherine Kaye of the ESTCP Office for providing support and funding for this project.

1. INTRODUCTION

1.1. Background

Unexploded ordnance (UXO) contamination is a high-priority problem for the Department of Defense (DoD). Recent DoD estimates of UXO contamination across approximately 1,400 DoD sites indicate that 10 million acres are suspected of containing UXO. Because many sites are very large (greater than 10,000 acres), the investigation and remediation of these sites could cost billions of dollars. However, on many of these sites only a small percentage of the site may in fact contain UXO contamination. Consequently, determining applicable technologies to define the contaminated areas requiring further investigation and munitions response actions could provide significant cost savings. Therefore, the Defense Science Board (DSB) has recommended further investigation and use of Wide Area Assessment (WAA) technologies to evaluate their utility in determining the actual extent of UXO contamination on DoD sites (DSB, 2003).

In response to the DSB Task Force report and recent Congressional interest, the Environmental Security Technology Certification Program (ESTCP) designed a Wide Area Assessment pilot program that consists of demonstrations at multiple sites. The purpose of the demonstrations is to validate the application of a number of recently developed and validated technologies as a comprehensive approach to WAA. These demonstrations of WAA technologies include deployment of high-altitude airborne sensors, helicopter-borne magnetometry arrays, and ground surveys.

This report documents the demonstration of the Helicopter Multi-sensor Towed Array Detection System (MTADS) Magnetometry (HeliMag) technology for the WAA of 5,020 acres at the former Pueblo Precision Bombing Range (PBR) #2. This demonstration was conducted as part of ESTCP project MM-0535.

HeliMag provides efficient low altitude digital geophysical mapping (DGM) capabilities for metal detection and feature discrimination at a resolution approaching that of ground survey methods, limited primarily by terrain, vegetation, and structural inhibitions to safe low-altitude flight. The magnetometer data can be analyzed to extract either distributions of magnetic anomalies (which can be further used to locate and bound targets, aim points, and open burn/open detonation (OB/OD) sites), or individual anomaly parameters such as location, depth, and size estimate. The individual parameters can be used in conjunction with target remediation to validate the results of the magnetometer survey.

1.2. Objectives of the Demonstration

The purpose of this demonstration was to survey a subset of the WAA demonstration site in areas amenable to low-altitude helicopter surveys. Specific objectives of this demonstration included:

- Identify areas of concentrated munitions, including the known and suspected target areas;

- Bound the target areas;
- Estimate density and distribution of munitions types and sizes;
- Characterize site conditions to support future investigation, prioritization, remediation, and cost estimation tasks.

A determination of success for this demonstration was based on the performance of the system, as described in Section 4.

1.3. Regulatory Drivers

This site and the associated target areas are classified by the United States Government as a Formerly Used Defense Site (FUDS) under the Defense Environmental Restoration Program (DERP). Currently, the WAA study area is undeveloped.

1.4. Stakeholder/End-User Issues

ESTCP managed the stakeholder issues as part of the WAA pilot program. ESTCP followed used a process that ensured that the information generated by the helicopter, water, and validation surveys is useful to a broad stakeholder community (e.g., technical project managers and Federal, State, and local governments, as well as other stakeholders).

2. TECHNOLOGY DESCRIPTION

2.1. Technology Development and Application

The Naval Research Laboratory (NRL) developed the MTADS technology. Use of this technology was transferred to Sky Research for commercialization via a Cooperative Research and Development Agreement (CRADA). Prior to the transfer, this technology was fully evaluated for the DoD by ESTCP (Nelson et al. 2005; Tuley and Dieguez 2005).

The HeliMag system includes a helicopter-borne array of magnetometers and software designed specifically to process data collected with this system and perform physics-based analyses on identified targets (Table 1). These technologies are described in greater detail in the following subsections.

Table 1. Sky Research HeliMag Technology Components

Technology Component	Specifications
Geophysical Sensors	7 Geometrics 822 cesium vapor magnetometers, 0.001 nanotesla (nT) resolution
GPS Equipment	2 Trimble MS750 GPS receivers, 2-3 centimeter (cm) horizontal precision
Altimeters	1 Optech laser altimeter and 4 acoustic altimeters, 1 cm resolution
Inertial Measurement Unit	Crossbow AH400, 0.1 degree resolution
Data Acquisition Computer	NRL Data Acquisition Computer
Aircraft	Bell Long Ranger helicopter

2.1.1. Helicopter Platform

Sky Research used a Bell Helicopter Model 206 helicopter (Figure 1) for data collection at the Pueblo PBR#2 site. The helicopter platform was used to deploy the geophysical sensors, global positioning system (GPS) equipment, altimeters, inertial measurement unit (IMU), and data acquisition computer (DAQ) technologies listed in Table 1. The helicopter is typically deployed at survey altitudes of 1-3 meters (m) above ground level (AGL).

An onboard navigation guidance display (Figure 2) provided pilot guidance, with survey parameters established in a navigation computer that shared the real-time kinematic GPS (RTK GPS) positioning data stream with the data acquisition computer. The survey course was plotted for the pilot in real time on the display. The sensor operator monitored presentations showing the data quality for the altimeter and GPS and the GPS navigation fix quality. This allowed the operator to respond to both visual cues on the ground and to the survey guidance display.

Following the survey, the operator has the ability to determine the need for surveys of any missed areas before leaving the site.

Figure 1. Helicopter MTADS technology as deployed on Bell Long Ranger helicopter.

2.1.2. Sensors and Boom

The MTADS magnetic sensors were Geometrics 822A Cesium (Cs) vapor full-field magnetometers (a variant of the Geometrics 822). The array of seven sensors was interfaced to NRL's DAQ and the sensors were evenly spaced at 1.5 m intervals on a 9 m Kevlar boom mounted on the helicopter. The boom used for this data collection was the NRL boom used in previous ESTCP demonstrations of the technology.

Figure 2. The track guidance system provides flight traverse information to the pilot.

2.1.3. Positioning Technologies

Two Trimble MS750 RTK GPS receivers were used to provide positions and platform attitude at 20 hertz (Hz), with four acoustic altimeters for recording the altitude of the platform. An IMU was used to correct for platform pitch. The data acquisition system was aligned with the GPS Universal Time Coordinated (UTC) time. The GPS time stamp was used as the basis for merging position data with sensor information.

RTK GPS was also used to generate positions for ground surveying. Sky Research utilized an in-house professional land surveyor to ensure that geospatial data generated by the project maintained accurate ties to the local coordinate system.

2.1.4. Data Acquisition System

Magnetometer, altimeter, and navigational instrumentation were streamed into a rack-mounted computer housed in the back seat of the helicopter (Figure 2). This computer ran a customized version of Geometrics MagLogNT data-collection software. The equipment rack also contained the GPS receivers and Geometrics G-822AS super counters, which controlled the sampling rates for the seven individual sensors. The magnetometer data are typically logged at 100 Hz, which provides a nominal down-the-track sample interval of 0.15 m at a typical survey speed of 15 m/second (m/s).

2.1.5. Data Processing

Data were downloaded via computer disks and uploaded via the Internet after each survey mission. Data processing was performed using custom application software running under the Oasis Montaj (Geosoft Ltd., Toronto, Canada) geophysical data processing environment. An overview of this process is outlined in the flow diagram provided in Figure 3. The processing conducted as part of this demonstration is described in greater detail in Section 3.6.5.

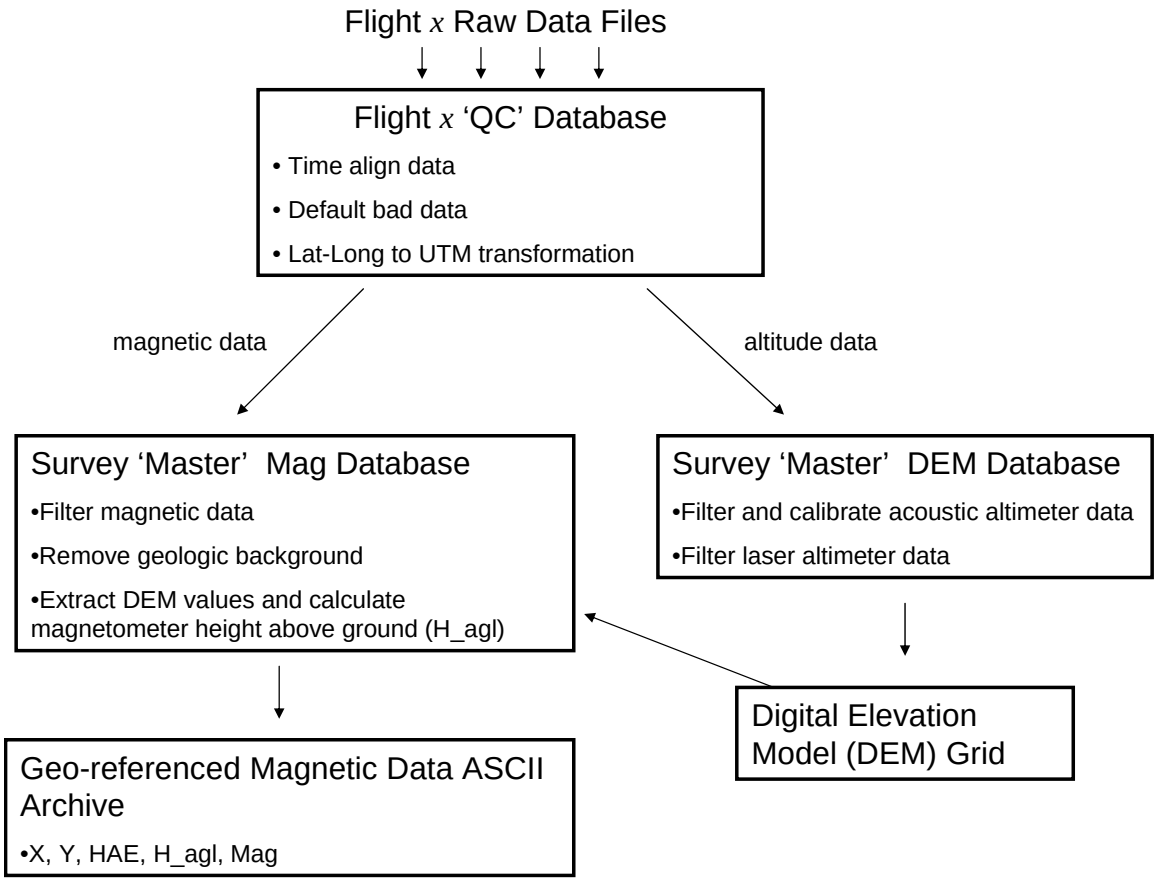

Figure 3. Helicopter MTADS processing flow chart.

2.1.6. Data Analysis

Once magnetic anomaly maps were created, anomalies were selected using an automated target selection methodology in Oasis Montaj. Automatic target selection for large-scale surveys such as this one has the advantage of being objective and repeatable as well as much faster than manual selection. However, automatic target pickers are not yet sophisticated enough to reliably detect closely spaced targets or targets that are at or below the same amplitude as local geologic signal. Therefore, to avoid selecting an excessive number of false targets, automatic target selection routines were only used to select targets with response amplitudes significantly above the background geologic noise. Furthermore, the automatic routines do not perform well in areas of high target density.

For the purposes of WAA where the main goal is to delineate target density throughout the survey site, the limitations of automatic target selection are not as detrimental as they would be if we were concerned with detecting every possible UXO target. The challenge is to calibrate the automatic target selection routine so that the number of valid targets of interest selected is maximized, while minimizing the number of targets selected due to geologic noise (or other noise sources). To achieve this, manual target selection results were compared with those obtained using an automated target selection routine over a representative subset of the survey

site. The results of the comparison were used to fine-tune the parameters for automatic target selection.

2.2. Previous Testing of the Technology

Previous testing of the helicopter magnetometry technology in general was supported by ESTCP (Nelson et al. 2005). The primary development objective was to provide a UXO site characterization capability for extended areas, while retaining substantial detection sensitivity for individual UXO. The system included data-collection hardware in the form of a helicopter-borne array of magnetometers, and software designed to process data collected with this system and to perform physics-based analyses on identified targets.

2.3. Factors Affecting Cost and Performance

For all airborne surveys, the largest single factor affecting the survey cost is the cost of operating the survey aircraft and sensors at the site. These equipment costs are related to capital value, maintenance overhead, and direct operating costs of these expensive sensor and aircraft systems. The cost of mobilization to and from the site increases with distance, and flexibility of scheduling is critical in determining whether mobilization and deployment costs can be shared across projects. In addition, helicopter surveys are limited by topography and vegetation and therefore can be employed only at sites with suitable conditions.

Another significant cost factor is data volume and the requirement for a robust data processing infrastructure to manage large amounts of digital remote sensing data. For this demonstration site, the WAA datasets (including orthophotography, Light Detection and Ranging [LiDAR], hyperspectral imaging [HSI], synthetic aperture radar [SAR] and ground transect datasets collected by other demonstrators) were managed in a geospatial database under a separate Sky Research demonstration project providing geospatial support to the overall ESTCP WAA pilot program under ESTCP MM-0537.

2.4. Advantages and Limitations of the Technology

As with all characterization technologies, site-specific advantages and disadvantages exist that strongly influence the level of success of their application.

Advantages of HeliMag technologies include:

- The ability to characterize very large areas;
- Lower per-area cost than ground-based DGM methods where complete areal coverage is required. Cost comparisons for ground-based transect surveys will vary depending on the level of coverage required.

Limitations of HeliMag technologies include:

- As a WAA tool, not intended to detect individual munitions and explosives of concern (MEC);
- Constraints on use due to site physiography, such as terrain, soils, and vegetation.

3. DEMONSTRATION DESIGN

3.1. Performance Objectives

Performance objectives are a critical component of the demonstration because they provide the basis for evaluating the performance and costs of the technology. For this demonstration, both primary and secondary performance objectives were established. Table 2 lists the performance objectives for the helicopter MTADS technology, along with criteria and metrics for evaluation.

3.2. Test Site Selection

The selection of the Pueblo PBR#2 demonstration site as one of several demonstration sites in the WAA pilot program was based on criteria selected by the ESTCP Program Office in coordination with the WAA Advisory Group of state and federal regulators.

3.3. Test Site History/Characteristics

Pueblo PBR#2 was used as a World War II-era military training facility, located in the southern part of Otero County, Colorado. Within the 105 square-mile (67,770 acres) FUDS, the WAA demonstration plan area consists of approximately 7,400 acres encompassing two documented bombing targets (Bombing Targets #3 and #4 [BT3 and BT4]) and a suspected 75-mm air-to-ground gunnery target area (Figure 4).

The physiography and known munitions use history of the study area are discussed in some detail in the conceptual site model (CSM) (Versar 2005). Physiographic and historic military use characteristics most relevant to the technology demonstration are described briefly in this report

Topography. The study area is rolling terraced terrain to the south dissected by several intermittent drainages. The northern half is traversed southwest (SW) to northeast (NE) by an eroded bedrock ridge with a dissected terrace to the northwest. BT4 is on the nose of a gentle rounded ridge, while BT3 is on a steeper slope below and east of the ridge. The suspected 75-mm air-to-ground target zone is in a multiple-drainage incised bowl draining the steepest part of the ridge.

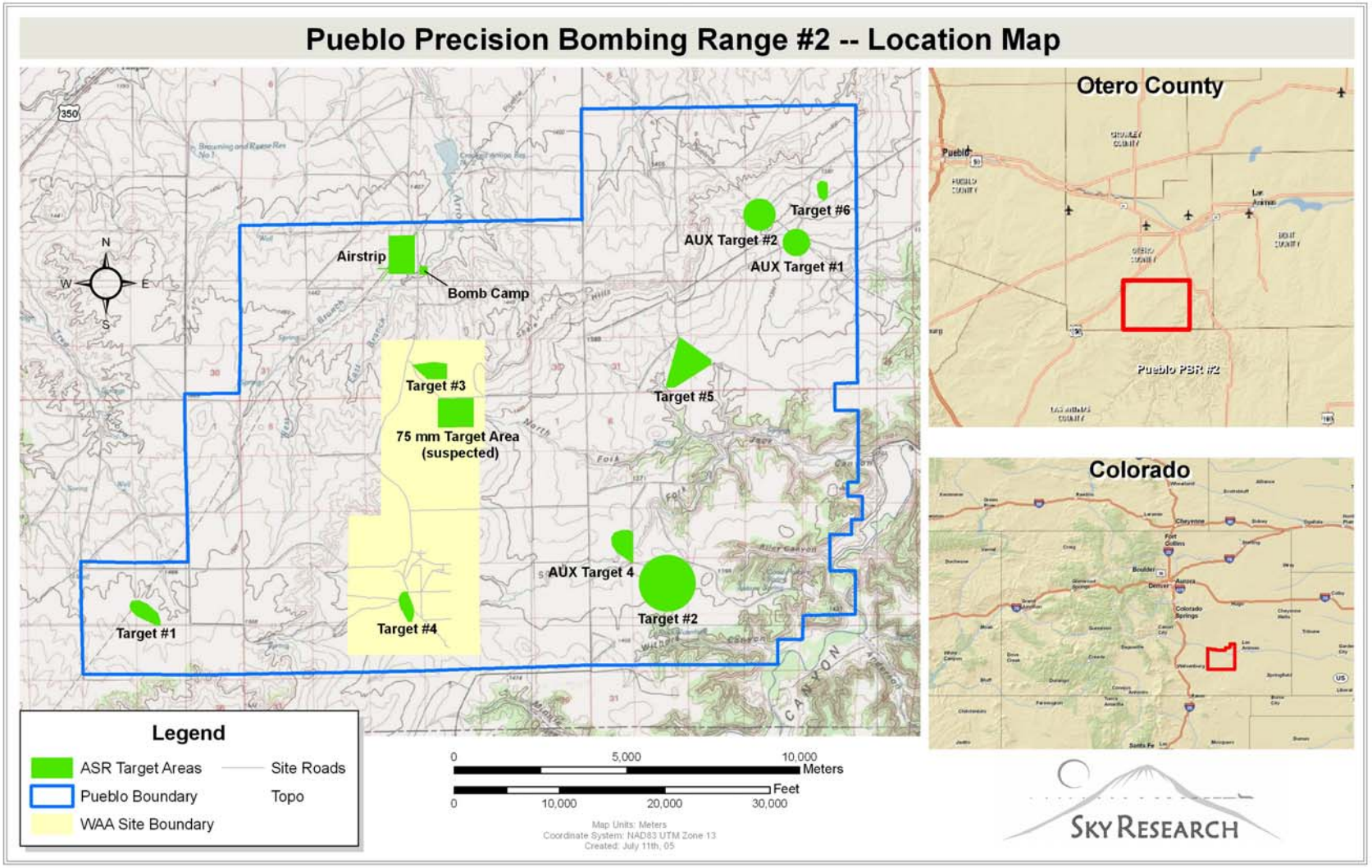

Figure 4. The WAA demonstration area (in yellow) is located within the former Pueblo PBR#2 in Otero County, Colorado.

Soils and Vegetation. The majority of the site is composed of deep silty sandy clays over silty clay subsoils, on gypsum, marl and limestone parent material. On the ridge, sedimentary bedrock is exposed with poorly developed colluvial soils on the associated slopes. The dominant vegetation is short- and mid-grass prairie dominated by buffalo grass (*Buchloe dactyloides*) and blue grama (*Bouteloua gracilis*), with a mixed overstory of taller native grasses including western wheatgrass and various needlegrass species. Many native forbs are present, and the most common non-herbaceous species include yucca, prickly pear, and cholla. Riparian zones along ephemeral streams on the site are vegetated with sparse riparian scrub and scattered cottonwoods with the understory largely barren due to cattle grazing.

Climate and Hydrology. The climate of the site is characterized by hot dry summers and cold winters. Some of the seasonal precipitation is from winter snows, but strong thunderstorms and associated erosion are the typical spring and summer precipitation pattern. Surface munitions and MEC in the vicinity of the suspected 75-mm air-to-ground target area and BT3 sites may be due to surface transport and burial by erosion and soil movement associated with these seasonal rainfall events. Similarly, micro-topographic target and impact features at these sites are most subject to obliteration by climatic factors.

Land Use. Land within the study area is primarily in Federal ownership managed by the U.S. Forest Service as the Comanche National Grasslands with portions leased to private owners or owned by the State of Colorado. Somewhat less than 2,000 acres of the entire WAA study area are privately-owned, non-residential gazing lands. Quite a number of stock tanks, wells, impoundments and associated access roads are present across the area to support grazing use. Some recreational use of the National Grasslands is cited in the CSM (Versar, 2005).

Former Munitions Use. The study area includes two documented bombing targets (BT3 and BT4) and one suspected 75-mm air-to-ground target area inferred from an unsubstantiated record of the presence of a single 75-mm armor-piercing tracer round documented in the Archive Search Report (ASR) (U.S. Army Corps of Engineers, 1995). The approximate locations of nine bombing targets were documented in the ASR, and the presence of an air-to-ground gunnery range plus submarine and ship skip bombing targets were documented but not located. Therefore, it was postulated prior to the demonstration that undocumented target locations could potentially lie within the study area.

Documented munitions present on the site surface within the study area includes AN-M30 and AN-M30-A1 General Purpose 100 pound (lb) bombs, M38A2 Mk15Mod3 100-lb practice bombs, 4-lb Incendiary Bombs, 50 caliber small arms rounds, and the single 75-mm AP cannon round. Air-to-ground rocketry by fighter squadrons stationed at La Junta Army Air Force (AAF) is documented in the ASR, however no documentation of the expected munitions type (possibly 2.25” practice or 5” high explosives [HE] rockets characteristic of the era) is provided in the findings.

Table 2. Performance Objectives

Type of Performance Objective	Primary Performance Criteria	Expected Performance (Metric)
Primary/Qualitative	Ease of use and efficiency of operations for each sensor system	Efficiency and ease of use meets design specifications
Primary/Quantitative	Geo-reference position accuracy	Within 0.25 m
Secondary/Quantitative	Survey coverage	>0.95 of planned survey area
Secondary/Quantitative	Operating parameters (altitude, speed, overlap, production level)	1-3 m AGL; 15-20 m/s (30-40 knots); 10%; 300 acres/day
Primary/Quantitative	Noise level (combined sensor/platform sources, post-filtering)	<1 nT
Secondary/Quantitative	Data density/point spacing	0.5 m along-track 1.5 m cross track
Secondary/Quantitative	MEC parameter estimates based on calibration strip results	Size <0.02 m; Solid Angle < 10º

3.4. Present Operations

There are no active military operations at Pueblo PBR#2. Site characterization activities are currently underway and are being conducted under the FUDS program.

3.5. Pre-Demonstration Testing and Analysis

As discussed previously, the helicopter technology utilized for this demonstration is based on the NRL MTADS technology, transferred to Sky Research for commercialization via a CRADA. Prior to the transfer, this technology was fully evaluated by ESTCP (Nelson et al. 2005; Tuley and Dieguez 2005).

3.6. Testing and Evaluation Plan

3.6.1. Demonstration Set-Up and Start-Up

Mobilization for this project required:

1) Mobilization of the equipment, pilot, and sensor operators.
2) Deployment of ground-support personnel to establish ground fiducials, establish and operate GPS base stations, establish calibration line location and collect data on calibration location, and provide logistical support.
3) Establishment of calibration line and standard pre-collection maintenance and calibration procedures established during previous deployments.

A base of field operations was established at the La Junta Municipal Airport, providing fuel and temporary hanger/storage space during operations at the site.

Ground Control

RTK GPS provided centimeter-accuracy real time positioning and was used with the HeliMag system. It was also used to generate positions for ground fiducials and for positioning ground calibration data and field verifications. The Sky Research in-house professional land surveyor ensured that geospatial data generated by the project maintain accurate ties to the local coordinate system.

Sensor Calibration Targets

A 350 m calibration lane, oriented north-south, was seeded with 8 targets comprising four unique types of items (Table 3). Calibration flights were flown at the start and end of each day of data collection, resulting in 22 datasets collected over 11 days over the calibration lane. Unfortunately, during the first few days the radio coverage for the RTK GPS corrections did not extend to the calibration line. Consequently, data that did not have high quality RTK position information have been rejected (consistent with the treatment of all of the survey data). In addition, it was discovered that the targets were frequently being disturbed by livestock. These problems were rectified after the first four days of survey production. Finally, it appears that one

of the 2.75" rockets (Target ID #2008) was mis-positioned (or moved by the livestock and not re-positioned) and does not appear in any of the survey calibration line passes. No targets were buried and no attempt was made to measure a probability of detection.

Table 3. Calibration Items Seeded in the Calibration Lane

ID	X	Y	Azimuth	Description
2001	617250.314	4178694.978	79º 25' 23"	Simulated 100-lb bomb
2002	617250.395	4178745.11	75º 22' 00"	Metal cache box
2003	617250.495	4178795.138	90º 45' 06"	155 mm projectile
2004	617250.26	4178844.979	100º 24' 10"	2.75" rocket
2005	617250.771	4178895.23	73º 14' 58"	Simulated 100-lb bomb
2006	617250.363	4178944.827	79º 28' 37"	Metal cache box
2007	617250.356	4178995.027	87º 05' 07"	155 mm projectile
2008	617250.198	4179029.887	82º 57' 12"	2.75" rocket

3.6.2. Period of Operation

Pre-planning for the demonstration survey was conducted in the summer of 2005, including submittal of the demonstration plan and final acceptance by the ESTCP Program Office. The ground surveys were conducted in early September prior to mobilization of the ground crew and helicopter to the survey site. The helicopter was mobilized from Denver, Colorado, and the field crew mobilized from Ashland, Oregon.

Data collection occurred from September 8 to 20, 2005, and was completed in 11 flight days; two days during the data collection time period were downtime for helicopter repair. The airborne survey crew consisted of one pilot and one system operator; a second airborne survey crew was added on September 15, 2005 to increase daily productivity. This allowed for an average productivity increase from 200-300 acres per day to 570+ acres per day, with productivity reaching 861 acres on September 17, 2005 (Table 4).

Table 4. HeliMag Data Collection at Pueblo PBR#2

Data Collection Day	Acres Surveyed
September 8, 2005	260
September 9, 2005	250
September 10, 2005	200
September 13, 2005	50
September 14, 2005	300
September 15, 2005	570
September 16, 2005	778
September 17, 2005	861
September 18, 2005	844
September 19, 2005	622
September 20, 2005	285
Acres Collected	**5,020**
Average Daily Productivity (acres/day)	**456.36**

3.6.3. Area Characterized

The HeliMag data collection area encompassed 5,020 acres of the WAA demonstration site (Figure 5). Figure 6 illustrates the combined HeliMag survey areas; the vertical scale represents the as-flown altitudes of the sensors (height above ground).

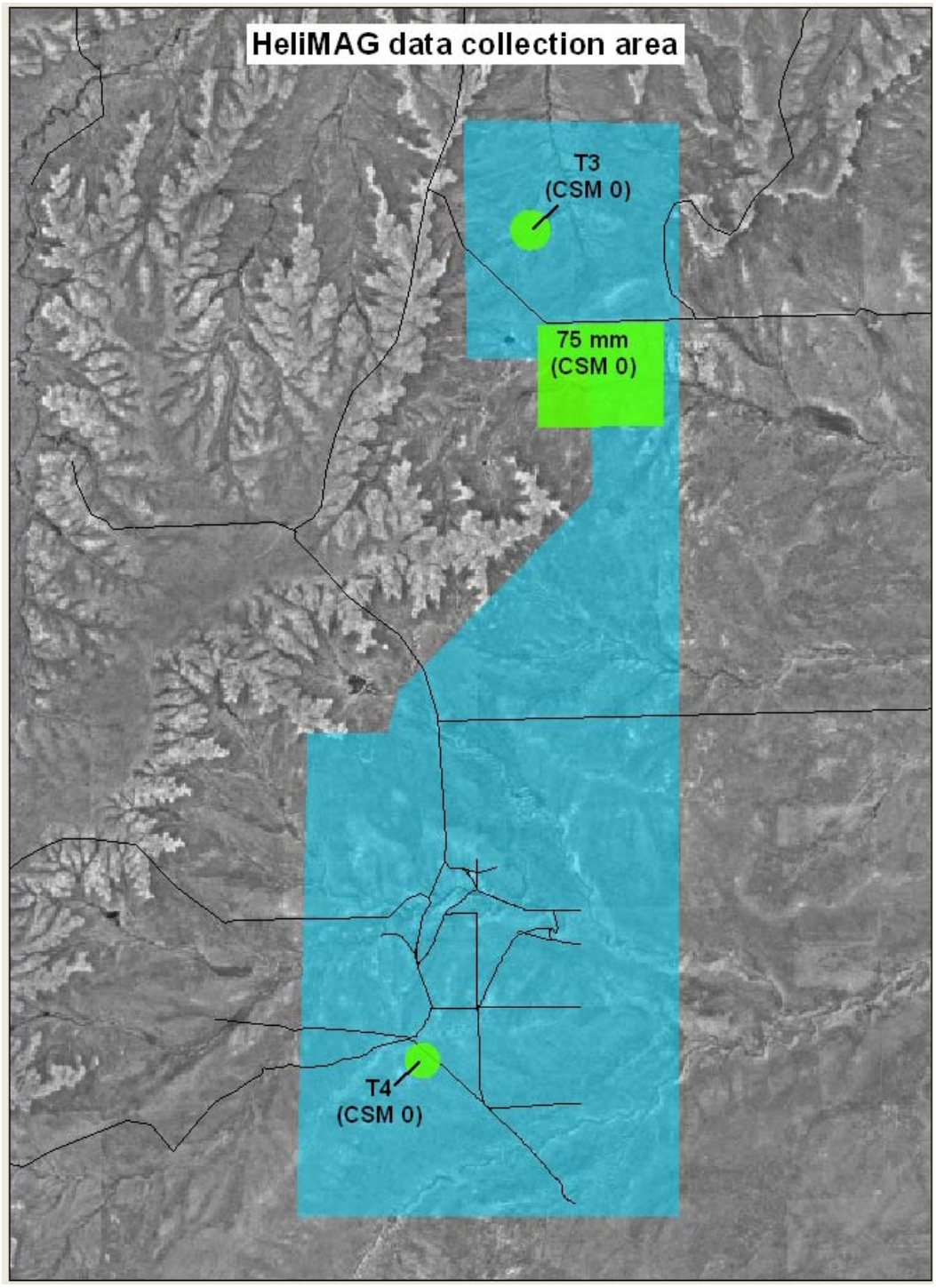

Figure 5. HeliMag data collection area at Pueblo PBR#2 WAA demonstration site.

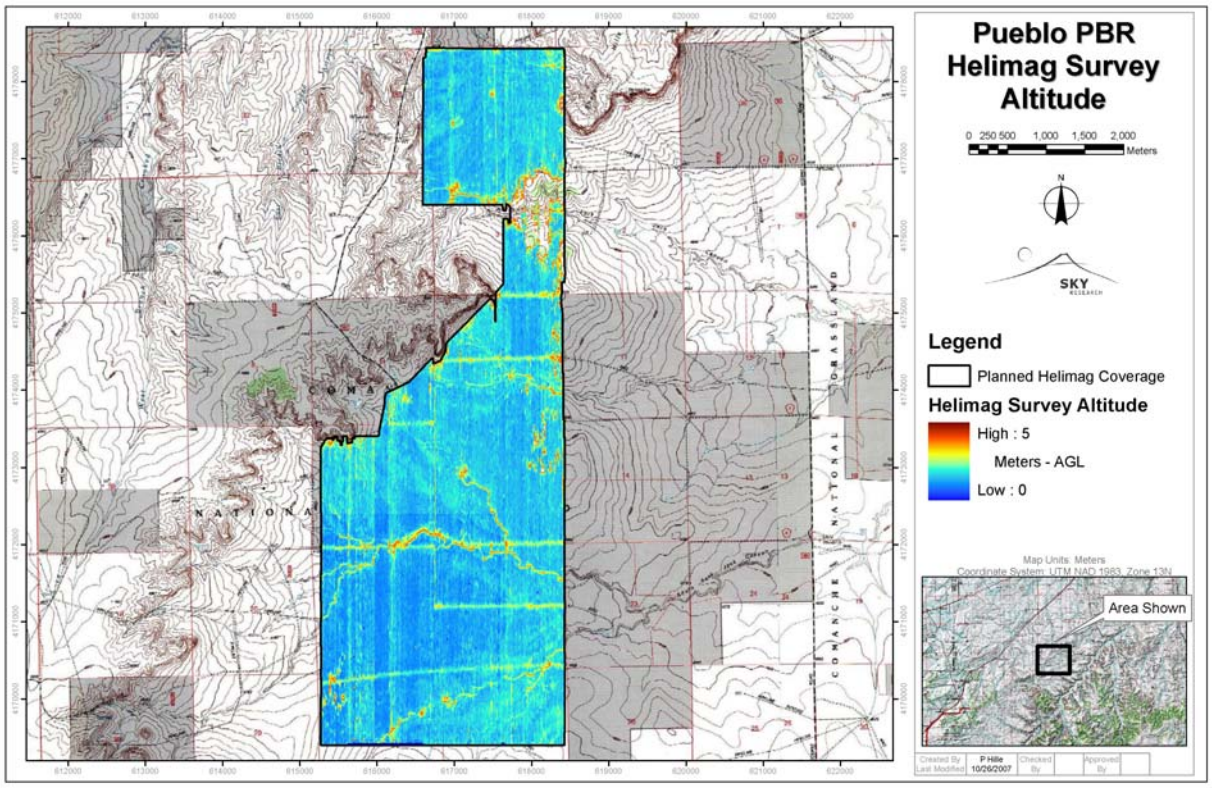

Figure 6. Map of as-flown HeliMag survey altitudes at Pueblo PBR#2.

3.6.4. Operating Parameters for the Technology

Sky Research deployed the airborne MTADS system on a Bell 206 Long Ranger helicopter platform, together with a pilot and system operator. A ground support team operated the RTK GPS base stations. The helicopter was flown at a low altitude (1-3 m), with a forward velocity of 10 - 20 m/s.

As described previously, seven full-field Cs vapor magnetometers were deployed on the 9 m boom mounted transversely on the front of the helicopter skids. The DAQ logged data at 100Hz. With the sensor spacing of 1.5 m and a speed over ground of 15 m/s, the resulting data density provides a minimum of 50 data points on a typical target to fit the dipole signature.

3.6.5. Data Processing

Data processing for this demonstration was performed by AETC. During the first data processing stage, the raw data for a given survey flight were time-aligned and transcribed from the various raw data files into a 'flight' database. Routines were run to automatically reject or 'default' invalid data. Data were rejected based upon status flags present in the raw data records or, in the case of the magnetometer data, a simple 'in range' (i.e. data with values outside of the 35,000 to

75,000 nT range were defaulted). test was used. The GPS geographic position coordinates were transformed to WGS84 Universal Transverse Mercator (UTM) coordinates. At this point the data were visually inspected to ensure both integrity and quality. This pre-processing stage is instrumentation-specific and the steps required to transcribe these data into a time-aligned database were dictated by the structure of the data outputs from each device and the manner in which they were logged. All data outputs were received by the on-board DAQ. A DAQ time stamp was appended to each sample data string and the sample was then stored in a separate data file for each device. Table 5 provides a list of the raw data input files generated during the demonstration.

Table 5. Helicopter MTADS Raw Data Input Files

Device	Sample Rate (Hz)	Data Type	Filename extension	Remarks
Geometrics custom DAQ computer system trigger	100	TTL pulse	TriggerDevice.trig	Generated and logged by the DAQ – initiates the magnetometer sampling
Geometrics Model 822A Cs Magnetometers	100	RS232-ASCII	822A.Mag_a / 822A_Mag_b	7 magnetometers are controlled by 2 consoles – Mag_A sensors 1-4, Mag_B sensors 5-7
Trimble Model MS750 GPS position/attitude data	20/10	RS232-ASCII	GPS.nmea	Position data are in Trimble GGK message format, azimuth and roll are in Trimble AVR message format
Trimble Model MS750 GPS PPS (pulse per second)	1	TTL pulse	PpsDevice.pps	Used to accurately align integer GPS time with DAQ time
Trimble Model MS750 GPS time tag	1	RS232-ASCII	SerialDevice.utc	Used to resolve the integer ambiguity of the GPS PPS signal
Optech Model 60 Laser Altimeter	10	RS232-ASCII	SerialDevice.laser	Measures helicopter height AGL
Crossbow Tilt meter	10	RS232-Binary	SerialBinDevice.tilt	Used primarily for aircraft pitch measurement
Fluxgate magnetometer	10	RS232-ASCII	SerialDevice.fluxgate	Provides redundant aircraft attitude measurement
Acoustic altimeters	10	Analog voltage	AnalogDevice.analog	Measures sensor array height above ground level at two points

An important consideration for integration of the positioning system with geophysical sensors is that of time alignment. For dynamic applications, the time of applicability (TOA) of the geophysical sensor data must be aligned with the TOA of the measured positioning data to within one millisecond. Any measurement will have some latency before the data are collected and stored, which may be static or variable in nature. In addition to this latency, conventional time stamping of RS232 data is not precise and can inject hundreds of milliseconds of additional delays. Thus, simply time stamping the positioning data as it is transmitted to the DAQ does not ensure that the TOA of the positions can be precisely aligned with that of the geophysical data. When the Geometrics magnetometer consoles are triggered externally, the time lag between this external trigger and the TOA of the magnetometer samples is constant. Thus, using a trigger pulse generated by the DAQ allows determination of the TOA of the magnetometer data relative to the DAQ system time.

GPS systems commonly have an internal latency that is variable (i.e., the time between the applicability of a given measurement and the transmission of the derived position will vary) in addition to the serial port variability. To allow users to know precisely when a measurement applies, the data message is time stamped (i.e., the position solution is given in 4 dimensions; time, x, y, and z) to a very high degree of precision. In addition, GPS receivers also output a pulse per second (PPS) trigger at every precise integer second to provide a means to synchronize the DAQ time with GPS time. The integer ambiguity of the PPS trigger is resolved by sending the data acquisition system a message (via RS232) that is simply used to assign the precise GPS integer time to the incoming PPS trigger. In this manner, GPS time may be precisely aligned with the DAQ system time.

The steps used to transcribe and time-align the raw data into a single flight database were as follows:

1) For each DAQ trigger event, the corresponding magnetometer data were read from the Mag_A and Mag_B files and stored as a database record. This record has seven magnetometer channels and a DAQ time channel.
2) The UTC time stamp was used to assign integer times to the GPS PPS data and these data were interpolated into a GPS time channel. This interpolation is based upon alignment of the DAQ time stamp assigned to each PPS with the existing DAQ time channel. This results in each sample of seven magnetometer readings having a corresponding DAQ time and GPS time record.
3) The GPS time channel and GPS time field in the raw data files were used to interpolate the GPS position and attitude data for each magnetometer sample. This results in the creation of the following channels in the database: Latitude, Longitude, Height above ellipsoid, GPS status, AVR yaw (angle of the sensor boom relative to true north), AVR roll (angle of the sensor boom relative to the horizontal plane), and AVR status. The geographic positions represent the positions of the master GPS antenna relative to the WGS84 ellipsoid. The GPS status and AVR status provide a quality of fit indication for the position and attitude data respectively.
4) The DAQ time channel and the DAQ time field in the raw data files were used to interpolate the ancillary data for each magnetometer record. The ancillary data channels include the following: laser, four acoustic altimeter channels (two for each acoustic altimeter station to provide redundancy), tilt meter pitch and roll, and fluxgate x, y, and z components.

After the data were transcribed, invalid data were defaulted to ‘dummy’ values. The magnetometer data were defaulted outside of a reasonable range and the GPS data were defaulted based upon the values of the two status flags. A four-point average filter was applied to the magnetometer data to remove the 25 Hz noise assumed to be vortex shedding. This noise is relatively small in amplitude (less than 0.5 nT) and, as a result, this filter has very little effect on the data.

Data processing with the use of Geosoft Oasis Montaj MTADS Processing Toolbox greatly speeds up the merging and data interpolating process due to the large database functionality and

optimized merging algorithms. Typical production processing for 300-500 acres takes approximately eight hours of data processing to produce a raw data plot image.

During each day of the demonstration, the project data processor conducted an initial review of the geophysical data to ensure that the data were within a reasonable range, free from dropouts/spikes and timing errors, and otherwise apparently valid. Oasis Montaj software performs the review and provides the mean, maximum, minimum, and standard deviation for each data file. The summary was reviewed and the data visually inspected. If any problems existed, the project geophysicist assessed the problem(s) and made adjustments to the field operations as needed to ensure quality data collection. Additional processing steps after the raw data processing step include filtering, geologic trend removal, and smoothing if needed.

3.6.6. Data Analysis

The use of an automatic target picking methodology was investigated as part of this demonstration. Automatic target selection for large scale surveys such as this one has the advantage of being objective and repeatable as well as much faster than manual selection if a very large number of targets are to be selected. However, automatic target pickers are not yet sophisticated enough to reliably detect closely spaced targets or targets that are at or below the same amplitude as local geologic signal. Furthermore these automated routines are not able to differentiate among our targets of interest, local geologic anomalies, and non-UXO-like cultural sources (e.g., pipelines). In practice, the decision to pick manually, or use an auto-picker then add/reject targets manually is made based upon the number of targets to be picked and the extent of geologic/cultural clutter.

To investigate the use of automatic target picking for the Pueblo PBR#2 demonstration, a comparison of the results of an automated target picking procedure versus manual target picking results was conducted over a representative section of the demonstration site (Figure 7). The final total magnetic field data were used to create Geosoft style grid images with a grid cell size of 1 m.

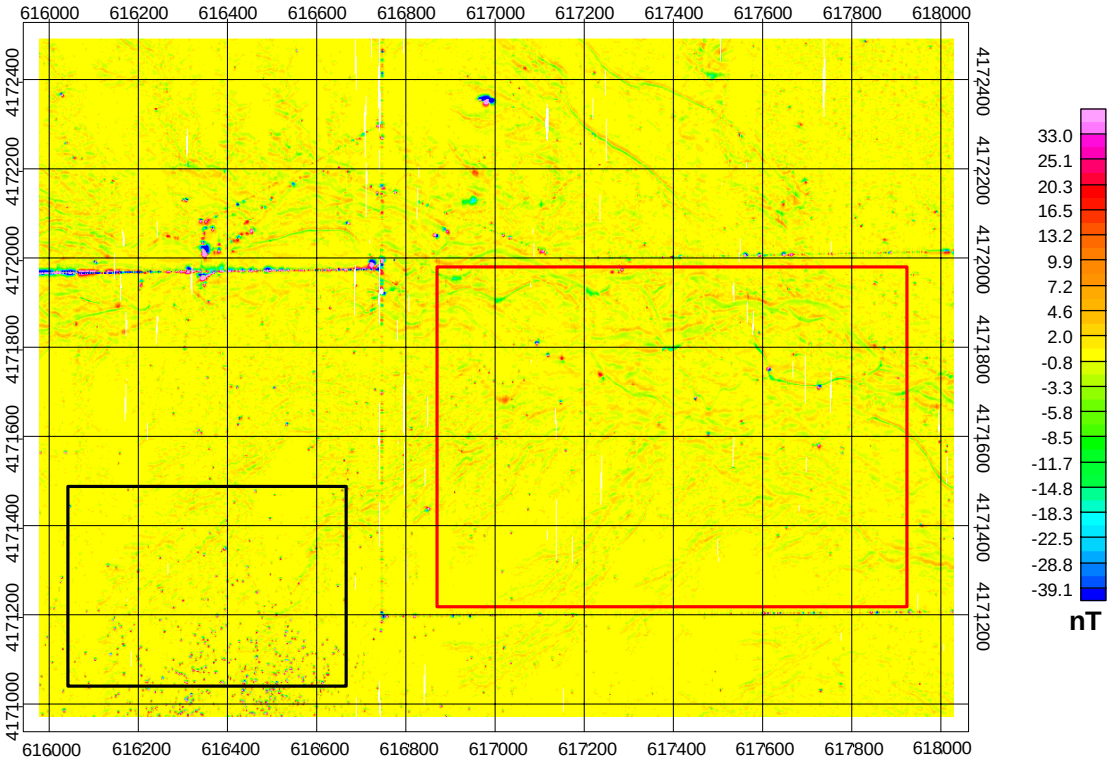

Figure 7. Sample areas used to calibrate the automatic anomaly picking routine, including areas with average geologic noise (black) and high geologic noise (red). The underlying image is a grid image of the total magnetic field.

The Geosoft peak detection utility was used as the automated target detection routine. This GX uses the Blakely method to find peaks in a grid (Blakely and Simpson, 1986). This algorithm compares the value of each grid cell with values of eight (8) nearest grid cells in four directions (along the row, column, and both diagonals). If the value of the grid cell in question is higher than its neighbors, it is assumed to be a target. This routine is calibrated through the use of two parameters: the number of filter passes performed on the grid (to remove high spatial frequency noise a 3x3 Hanning filter may be applied a user-selectable number of times) and the minimum amplitude threshold below which no peaks are selected. Because of the dipolar nature of the total magnetic field response of our targets of interest, the total magnetic field grid was converted to a magnetic analytic signal grid. The analytic signal is the square root of the sum of the squares of the derivatives in the x, y, and z directions, and as such, results in a single peak anomaly over our targets of interest.

The Geosoft peak detection routine was run a number of times while varying the detection threshold (from 2 to 9 nT/m) and the number of passes of a 3x3 Hanning filter (from 0 to 3). The results from these tests were compared with the results obtained using manual target detection.

Figure 8 shows the total number of targets selected using each method for each area and the sum of the two areas. The total number of targets is plotted as a function of the cut-off threshold used.

A separate curve is used for each number of filter passes as well as for the manual method. The curve for the manually selected targets was determined by sampling the analytic signal grid, based upon the original manually selected coordinates, then binning the targets accordingly.

At relatively high threshold values, the automatic target selection curves are similar to the manual selection curve (with the exception of the zero filter passes curve – clearly a minimum of one filter pass must be used). As the threshold is reduced below 5 nT/m (the point where the manual picker is marginally able to differentiate targets from geologic responses) the manual curve diverges radically from those of the automatic target selection routine. Using three filter passes does not appear to improve the auto-picker performance at lower thresholds (note that for each successive filter pass, the peak value for any given anomaly is reduced) and actually provides poorer performance at higher thresholds.

To provide an indication of the number of false target selections (relative to the number of true selections) as a function of target threshold, Figure 9 shows the total number of targets selected by the auto picker normalized by the number of manual picks as a function of cut-off threshold.

Finally, to provide an indication of the number of false anomaly selections as a function of anomaly threshold, Figure 10 shows to the total number of anomalies selected by the auto picker normalized by the number of manual picks as a function of cut-off threshold.

Based upon the data presented above and the calibration line results, the appropriate parameters used for the automatic anomaly selection algorithm were two filter passes with a cut-off threshold of 4.5 nT/m. These parameters minimize the effect of geology on the anomaly density map while at the same time maximize the number of valid anomalies selected.

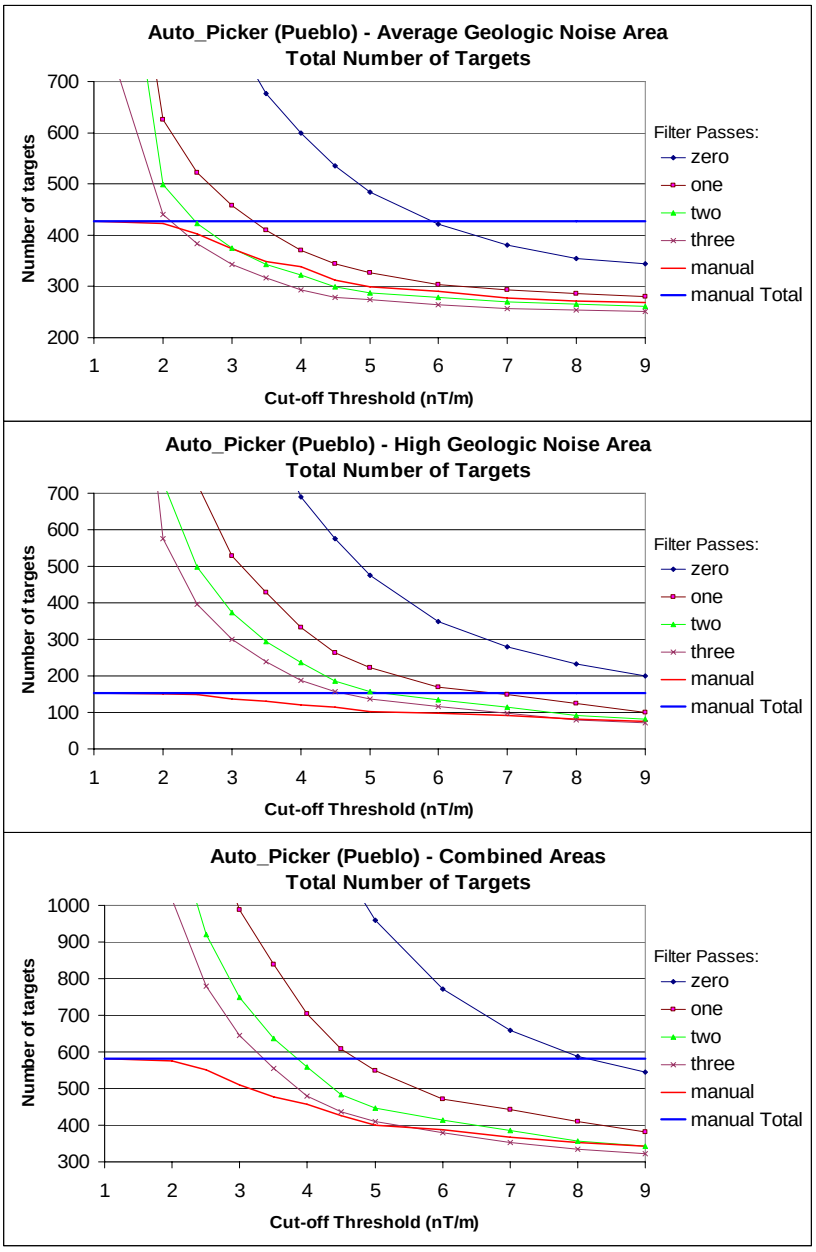

Figure 8. Total number of selected anomalies as a function of cut-off threshold amplitude.

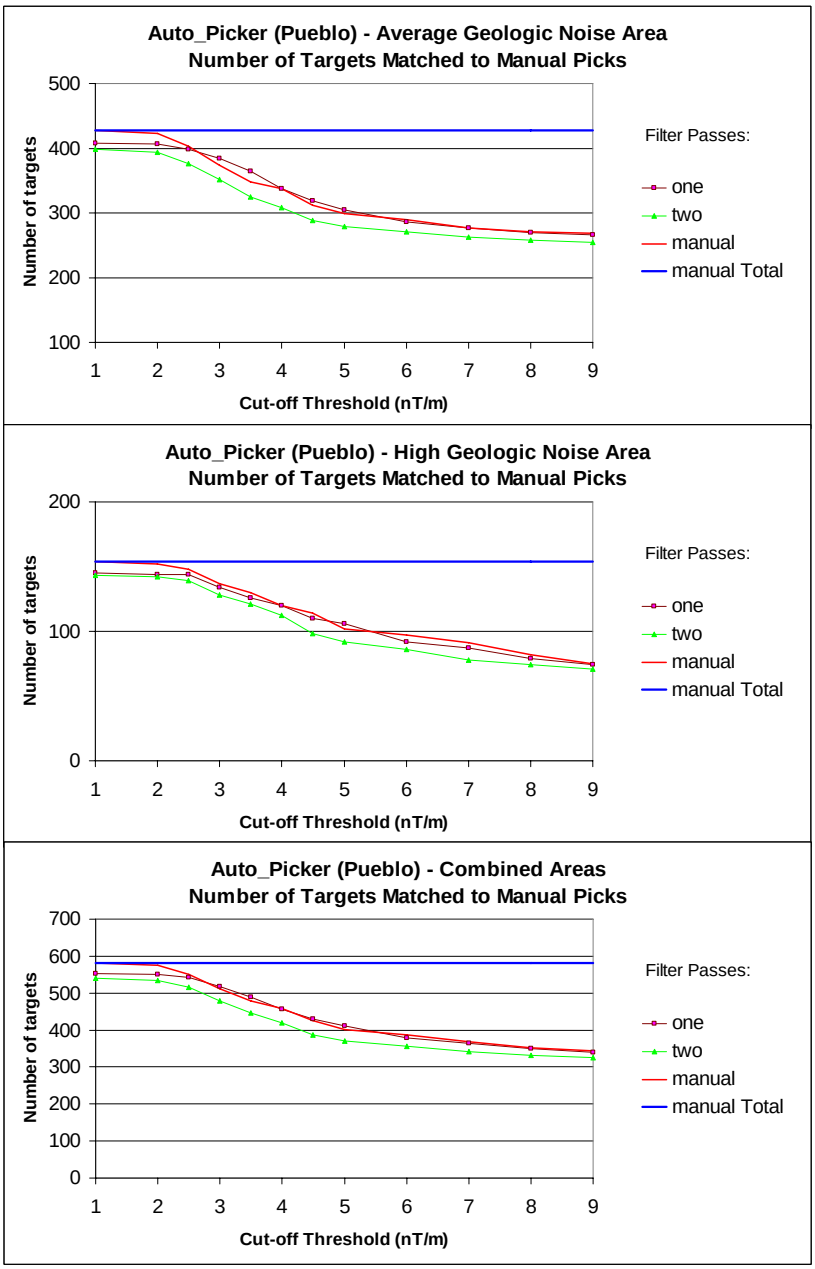

Figure 9. Number of valid anomalies selected as a function of cut-off threshold.

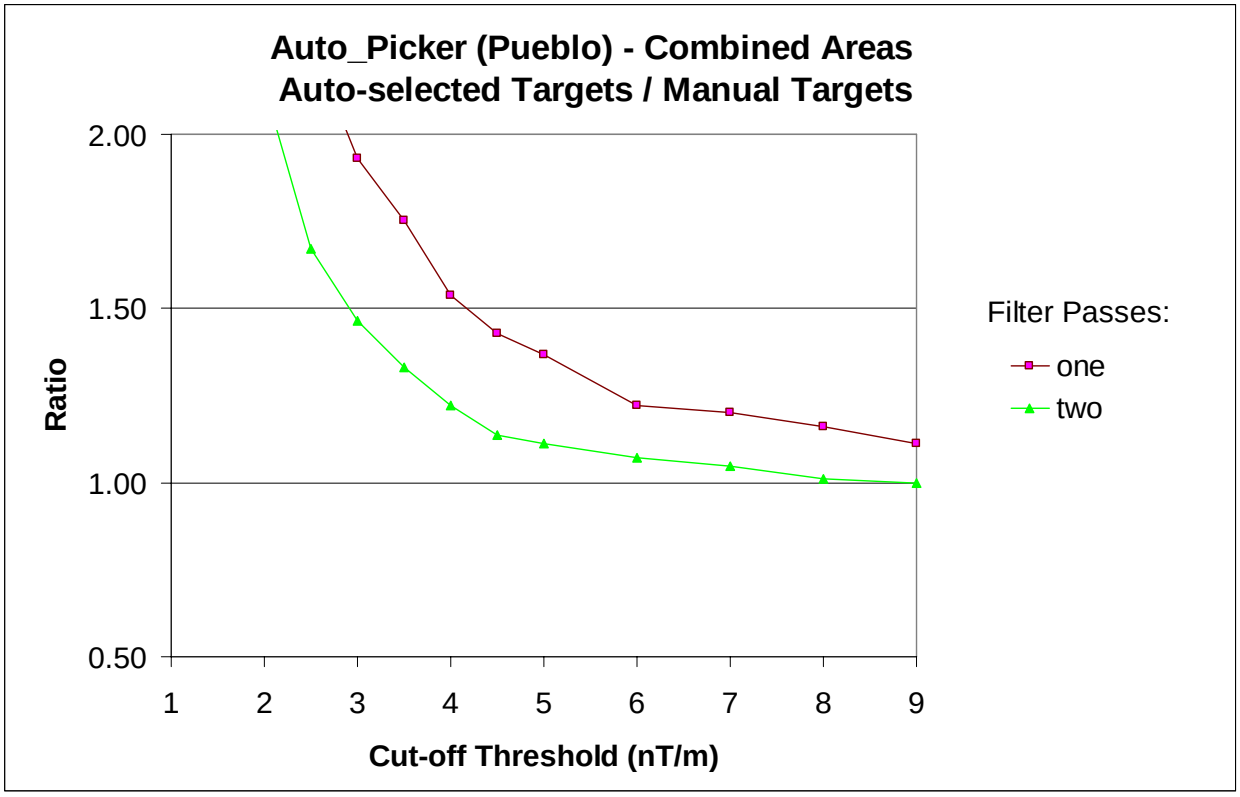

Figure 10. Number of anomalies selected automatically normalized by the number of manually selected anomalies as a function of cut-off threshold amplitude.

3.6.7. Demobilization

At the conclusion of the surveys, the helicopter, associated equipment, and field crews were demobilized from the site. Targets were investigated at a later date by a different contractor as part of the WAA validation surveys conducted on behalf of ESTCP.

4. PERFORMANCE ASSESSMENT

4.1. Data Calibration Results

4.1.1. Data Calibration

The data collected over each target from the calibration line passes that are assumed to be valid (i.e., target positions are stable and data positioning quality is good) were analyzed with the MTADS dipole fit algorithm (using the UX Analyze environment). This analysis derives the parameters for a model dipole that best fits the observed data. These parameters include horizontal position, depth, size, and solid angle (i.e., the angle between the Earth's magnetic field vector and that of the dipole model). The derived parameters were examined for accuracy (determined as the average error where relevant) and repeatability (indicated by the standard deviation), as presented in Table 6.

Table 6. Calibration Results for Calibration Lane Targets

Dipole Fit Parameter	Bias	Standard Deviation
Easting	n/a	0.16 m
Northing	n/a	0.07 m
Depth	0.39 m	0.19 m
Size	n/a	11 mm
Solid Angle	n/a	7.0 º

Under normal circumstances, the position accuracy would be very easy to determine and very relevant to any discussion of the system performance. However, it appears that the ground truth coordinates supplied for each target are not reliable. This is probably because the target positions were not re-established after it was found that the targets were moved by the livestock. For example, the positions for each target appear to have a repeatable bias (Figure 11). In Figure 12, the derived positions for each target with the bias removed are shown. The increased noise in the easting is assumed to be a result of the relative sample densities for each direction (calibration lines were flown in a north-south direction and along-track sample density is 5 to 10 times higher than for across-track).

4.1.2. Calibration Item Response

In the dipole fit depth estimates (Figure 13) it appears that the depths are too deep by an average of 0.39 m. Furthermore, the variability in the size estimates is a little greater than would be expected. Any errors in the sensor height above ground measurement will propagate into our depth estimate. The sensor height above ground was determined solely through the use of the acoustic altimeters. There is one altimeter mounted directly under each GPS antenna and thus these altimeters are positioned using only the RTK GPS system. This means that the observed bias must be due to a bias in the acoustic altimeter measurements. This bias is most likely due to

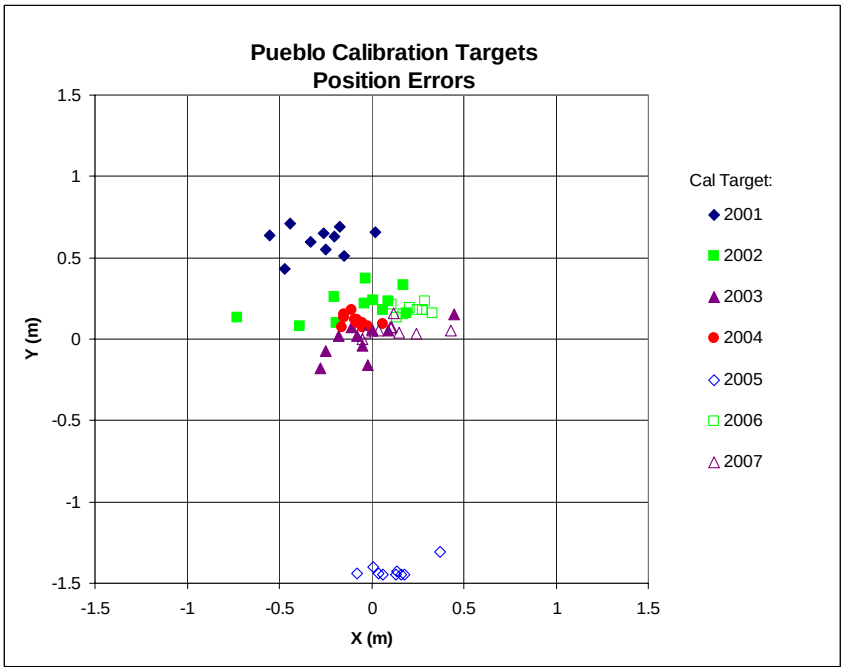

Figure 11. Derived x and y coordinates for the calibration targets relative to the supplied ground truth.

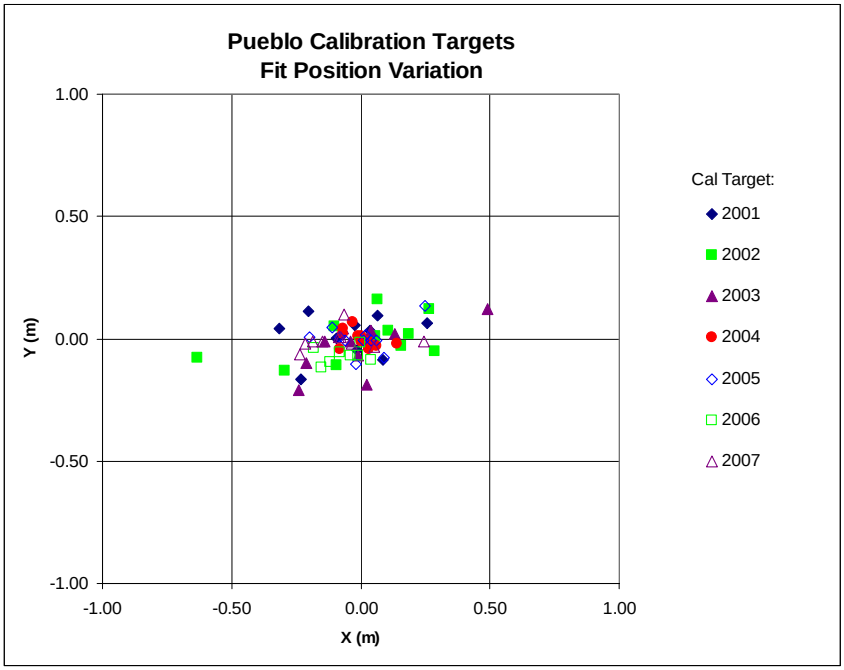

Figure 12. Derived calibration target positions with bias removed.

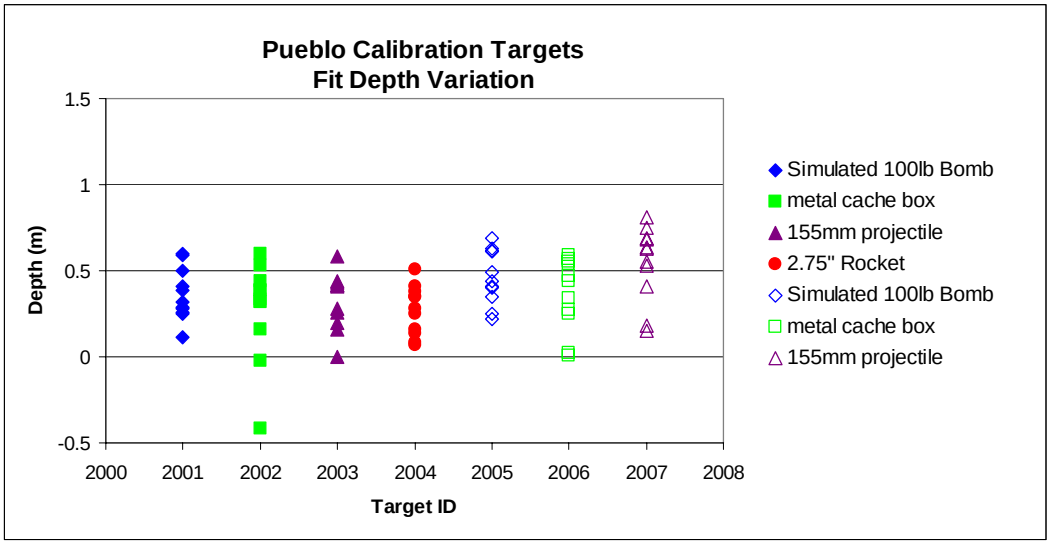

Figure 13. Dipole fit depth estimates for calibration line targets.

the grassy vegetative cover over the calibration area. This cover was reported to be approximately 18 inches (45 cm) high.

The dipole fit size estimate for any given munitions will vary considerably depending upon the alignment of the object with the Earth's magnetic field. Therefore, the size can only be used as a coarse estimate of the object size. For this reason, the accuracy of the size estimate of the calibration items is not of particular import when discussing the system performance, other than simply verifying that the estimate falls within the expected range for a given target (which they do, as shown in Figure 14). Because the calibration data consists of repeated flights over the same stationary targets, the repeatability of the derived size estimates can be used as an indication of consistent system performance. The average size for each specific target was removed from the target size estimates before the standard deviation for the entire set of size estimates was calculated.

In a manner similar to the size estimates discussed above, the dipole fit solid angle estimates depend heavily on the orientation of the target relative to the Earth's magnetic field. In the case of the calibration line test targets, the 'ground truth' is unknown and not really important. However the stability of this prediction for repeated flights over the calibration line is indicative of the performance of the airborne system (Figure 15).

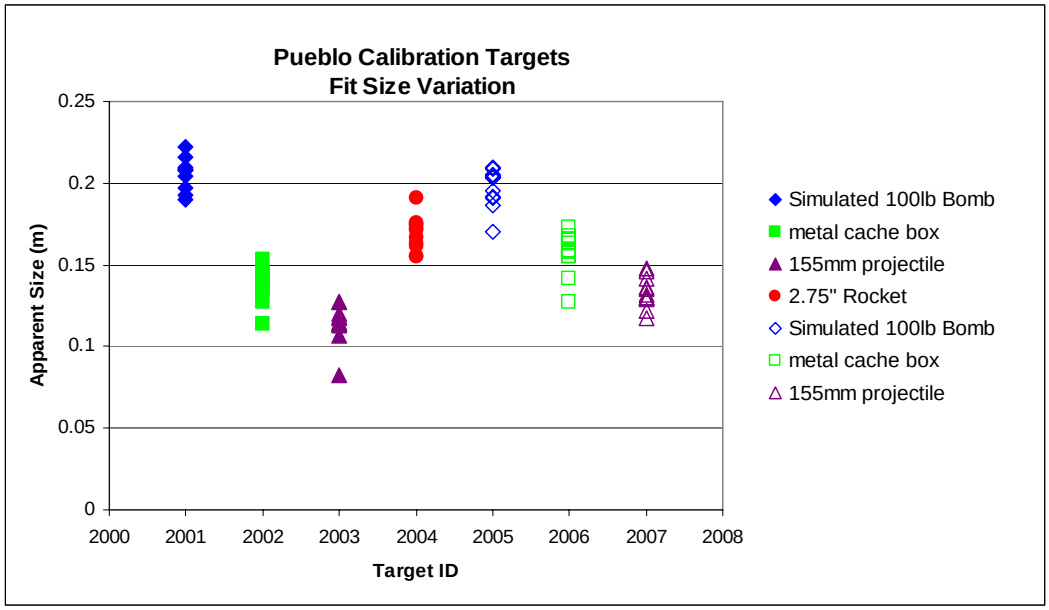

Figure 14. Dipole fit size estimates for calibration line targets.

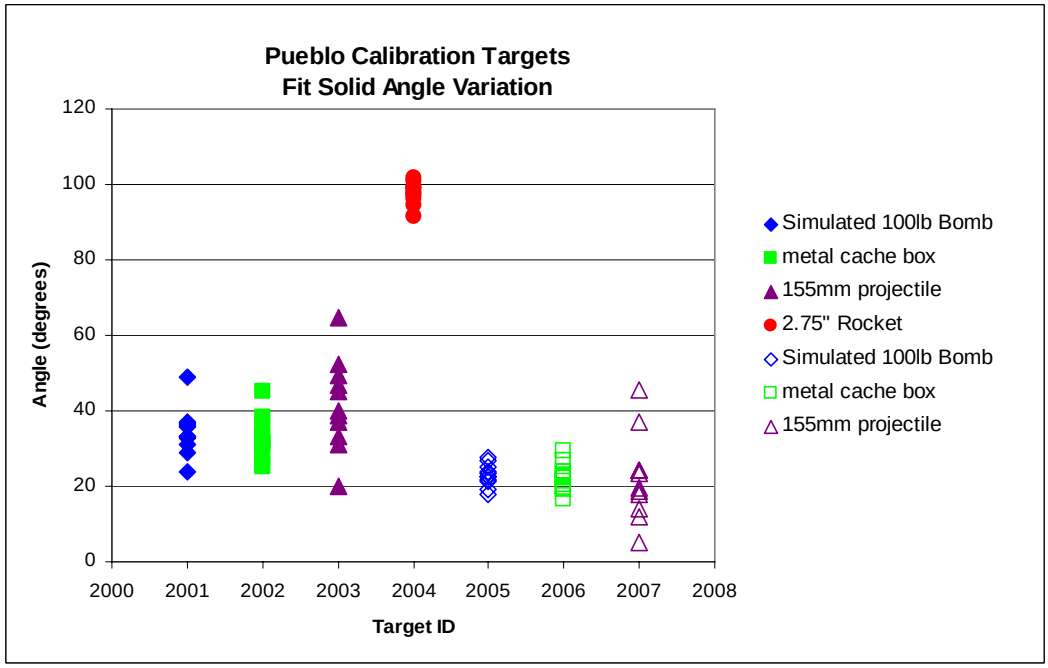

Figure 15. Dipole fit solid angle estimate for calibration line targets.

In addition to determining the repeatability of analyses performed on the calibration targets, the data collected over the targets can also be used to confirm the utility of the automatic target picking routine that is employed on the data sets to derive target density maps. The automatic target picker performs peak detection on a Geosoft style grid of the magnetic analytic signal that is in turn derived from a grid of the total magnetic field data. Prior to producing the analytic

signal grid, the total magnetic field data were upward continued by 0.75 m to simulate burial of the targets by the same amount. The peak detection algorithm first applies a 3 x 3 Hanning filter to the analytic signal grid to remove very high spatial frequency features (local noise) so that multiple peaks are not detected in the vicinity of a true peak. The number of applications of this filter is optional. A second parameter used is the minimum threshold for peak detection. Testing of this peak detection routine (described in Section 3.3.2) has shown that the optimal number of filter passes is two and the nominal threshold value should be around 5 nT/m. Figure 16 shows the peak amplitudes for multiple passes over the calibration targets.

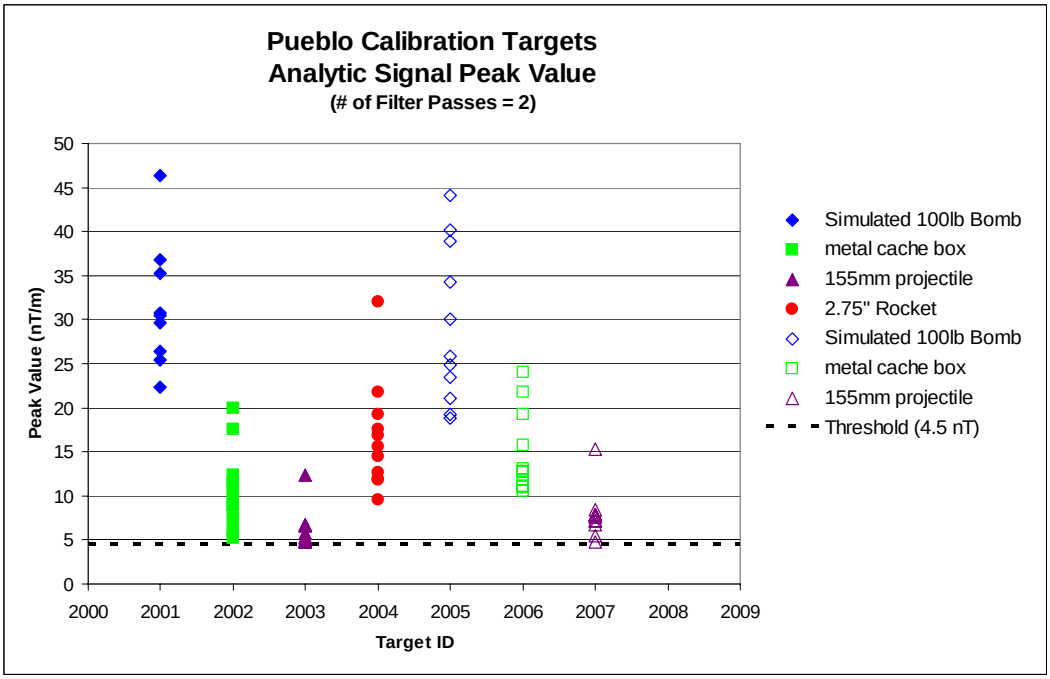

Figure 16. Peak analytic signal response for the calibration line targets.

4.2. Anomaly Picking Results

Using the automated picking methodology described in Section 3.6.6, 12,735 anomalies were selected from the data to assess the distribution of metal objects across the study area. Figure 17 illustrates the locations of these anomalies over the WAA study area.

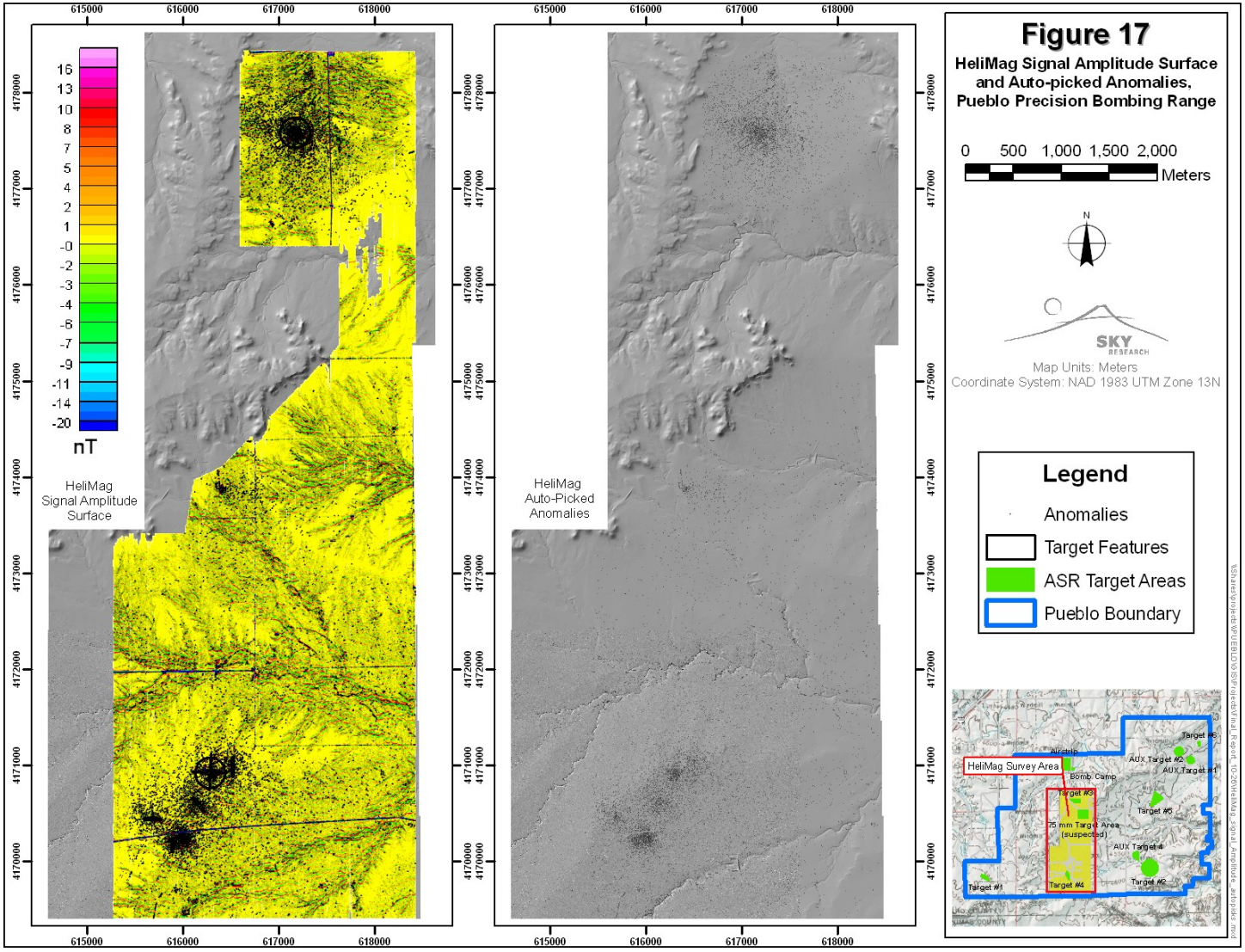

Figure 17. HeliMag amplitude surface interpolated from the filtered datapoints (left) and 12,375 auto-picked anomalies (right).

4.2.1. Metal Density Analysis

To visualize the distribution of metal objects across the study area, a density raster was computed using a 75 m radius neighborhood kernel that assigned anomaly densities in anomalies per hectare to each cell in the raster. Simply described, at grid nodes of every two meters the number of targets that appear within a 100 m search radius were counted. This search radius provides the density in targets per 31,416 m^2. These values were then 'normalized' by diving by 3.1416 to provide density estimates in targets/hectare. The resulting data were gridded to provide anomaly density images. At this site, the geologic response is benign and does not have the same amplitude and spatial distribution as responses attributable to discrete ferrous objects. For this reason, we can confidently assume that effectively all selected anomalies are attributable to discrete ferrous objects, thus the anomaly density is equivalent to the metal density

Figure 18 shows the metal density analysis computed from HeliMag anomalies, in relation to the BT3 and BT4 Target features detected in the LiDAR and orthophotography datasets (Sky Research, 2007). In each of these regions the ship targets and aiming circles coincide with significant elevations of magnetic anomaly density derived from the HeliMag data. The HeliMag results provide strong corroborating evidence supporting the existence of the additional 'ship' targets near BT4 that were not part of the original CSM.

Although scattered anomalies were detected within the suspected 75-mm Target area, a clearly defined high anomaly density area was not identified. However, a significant portion of the area was not surveyed at a low enough altitude to detect 75-mm munitions, so these areas have been masked out of the final results (Figure 19). Any definitive conclusions cannot be drawn from these data without corroborating evidence from ground truth investigations. However, in corroboration with the other WAA data sets, it is clear that no range exists.

Additional munitions response features identified in the high airborne datasets included an area north of BT3, a berm in the east central area of the demonstration site, and a barn or other ranching structure in the west central area of the demonstration site (Figures 20-22). Based on review of the HeliMag data, these areas show slight elevations in anomaly density (or no elevation at all in the case of the berm). None of these densities were consistent with high concentrations of MEC.

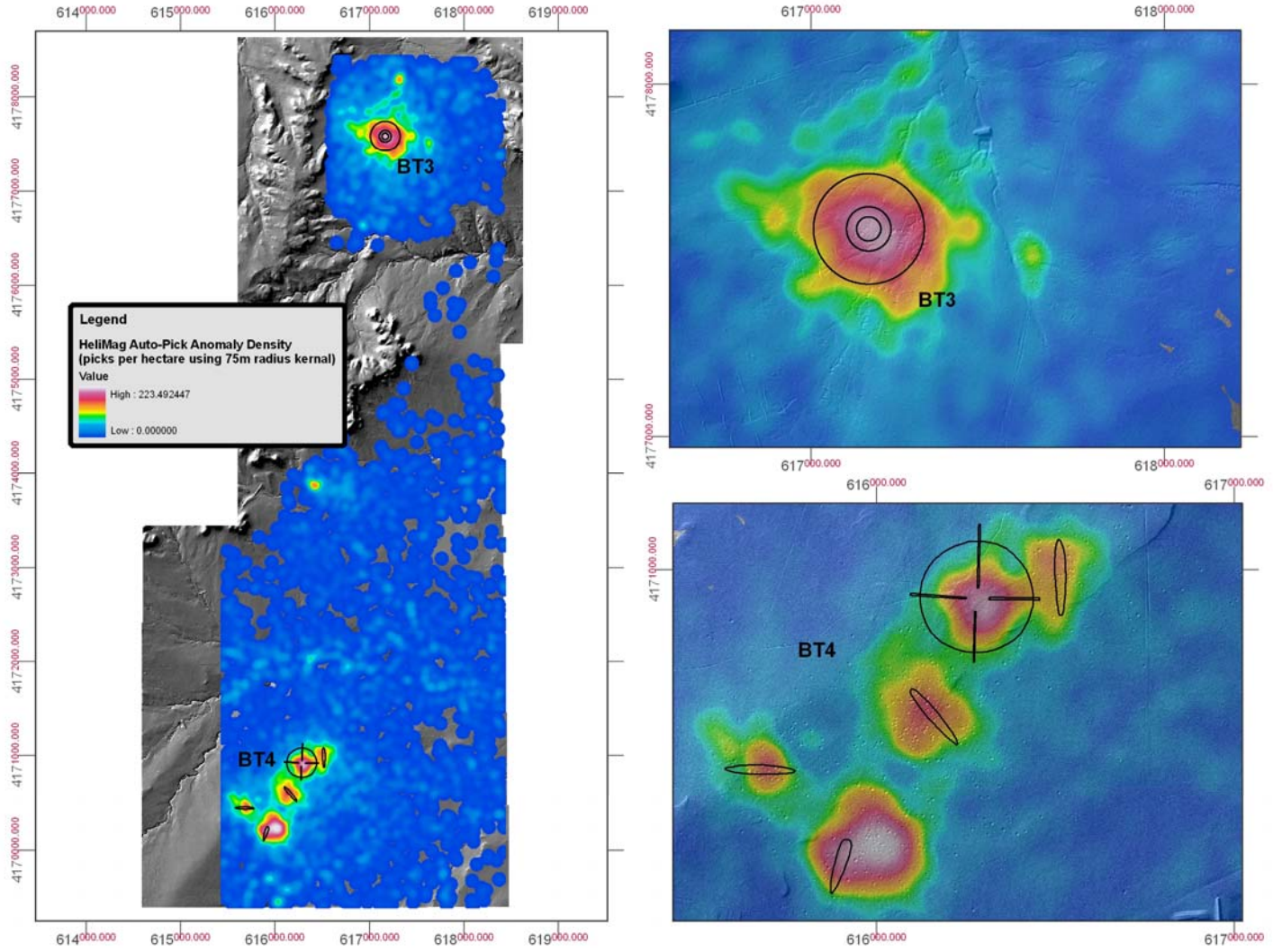

Figure 18. HeliMag anomaly pick density surface (anomalies per hectare) with enlarged density images over the two suspected bombing targets. Density surfaces are semi-transparent over the LiDAR data.

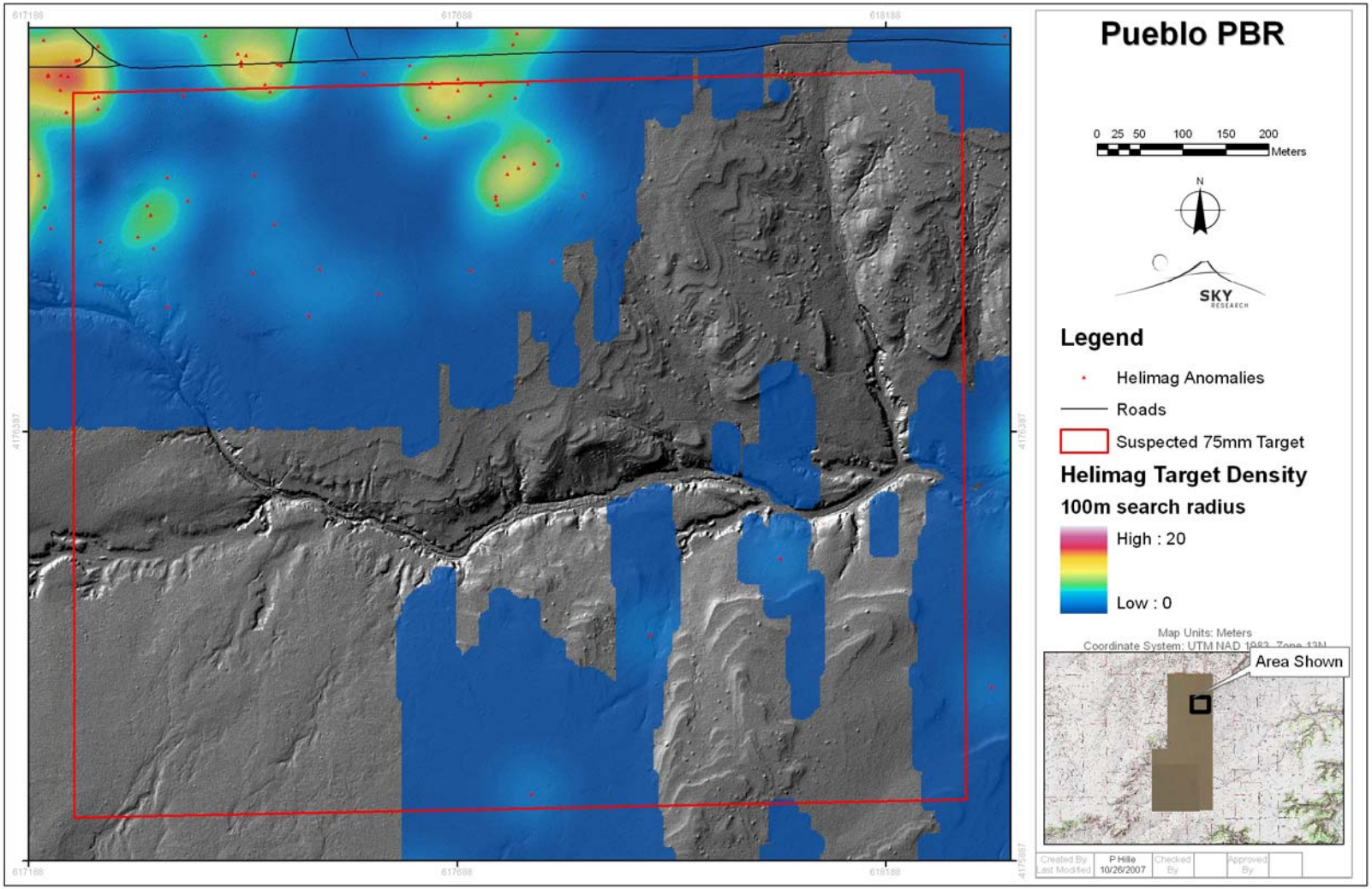

Figure 19. **HeliMag density analysis results from the suspected 75-mm Target Area. Density surfaces are semi-transparent over the LiDAR data.**

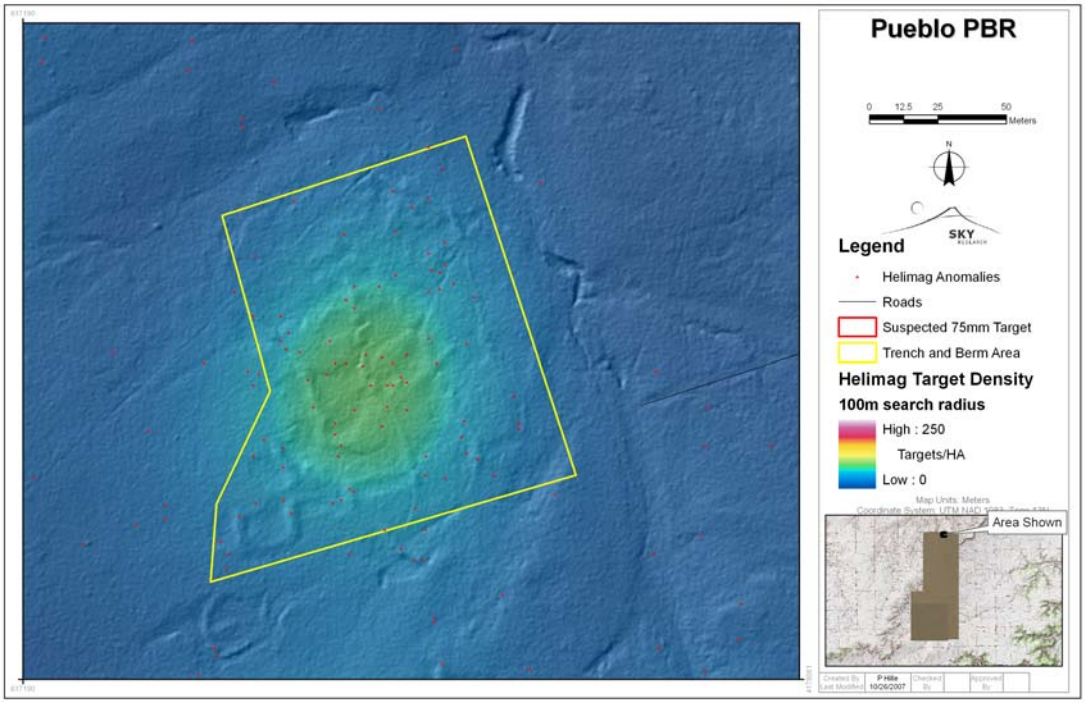

Figure 20. Target density results in area north of BT3 identified as a potential munitions related feature in the high airborne datasets. Density surfaces are semi-transparent over the LiDAR data.

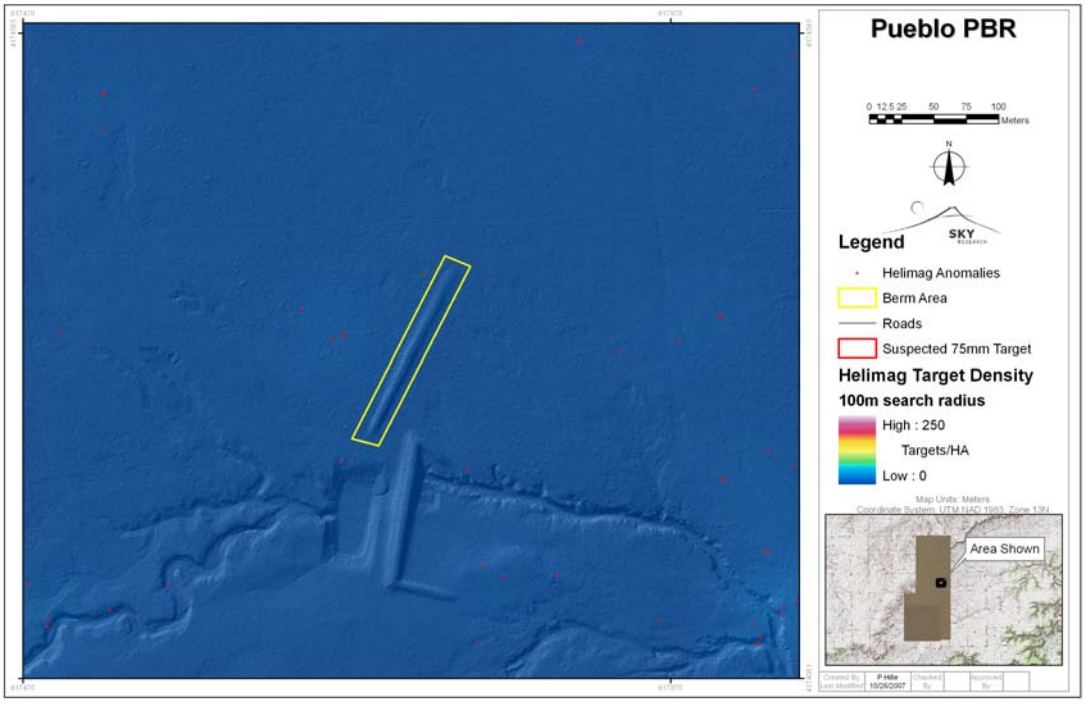

Figure 21. Target density results for berm feature identified as a potential munitions related feature in the high airborne datasets. Density surfaces are semi-transparent over the LiDAR data.

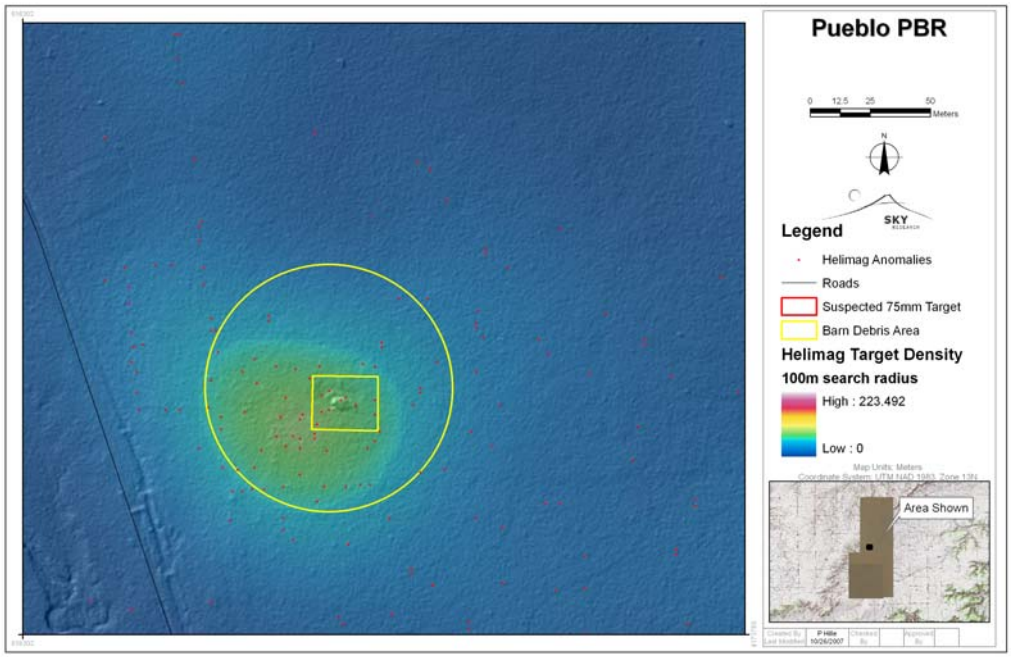

Figure 22. Target density results for the 'Homestead' area around a structure (most likely ranching related) identified as a potential munitions related feature in the high airborne datasets. Density surfaces are semi-transparent over the LiDAR data.

4.2.2. Target Dipole-Fit Analyses / Intrusive investigations

A subset of anomalies in each of the areas of interest was analyzed using the dipole fit analysis described in Section 4.1.1. These fit results were used to down-select candidate targets for intrusive investigation. Although a range of target sizes were picked, this subset of targets may not be entirely representative of a typical cross section of targets in these areas. Additionally in some areas the pick threshold approached the geologic noise levels, resulting in a high number of 'no-finds'. In Table 7 we summarize the number of anomalies analyzed in each area as well as the number of targets that were investigated intrusively.

Table 7. Targets selected for advanced analysis and intrusive investigation.

Area	Number of anomalies analyzed	Number of anomalies investigated
3C	62	6
1A	64	10
3B	172	9
Homestead	57	0
Simmons	54	54

Area	Number of anomalies analyzed	Number of anomalies investigated
South Target Circle	240	55
Ships (T4-AOI-3)	83	26

In Figure 23 we show the locations of each of the sub-areas identified in Table 7. Note that the only areas associated with high anomaly densities were the two areas associated with BT-4 (the BT4 'Target Circle Area' and 'Ship Area' (T4-AOI-3)) and, to a much lesser extent, the 'Homestead' area.

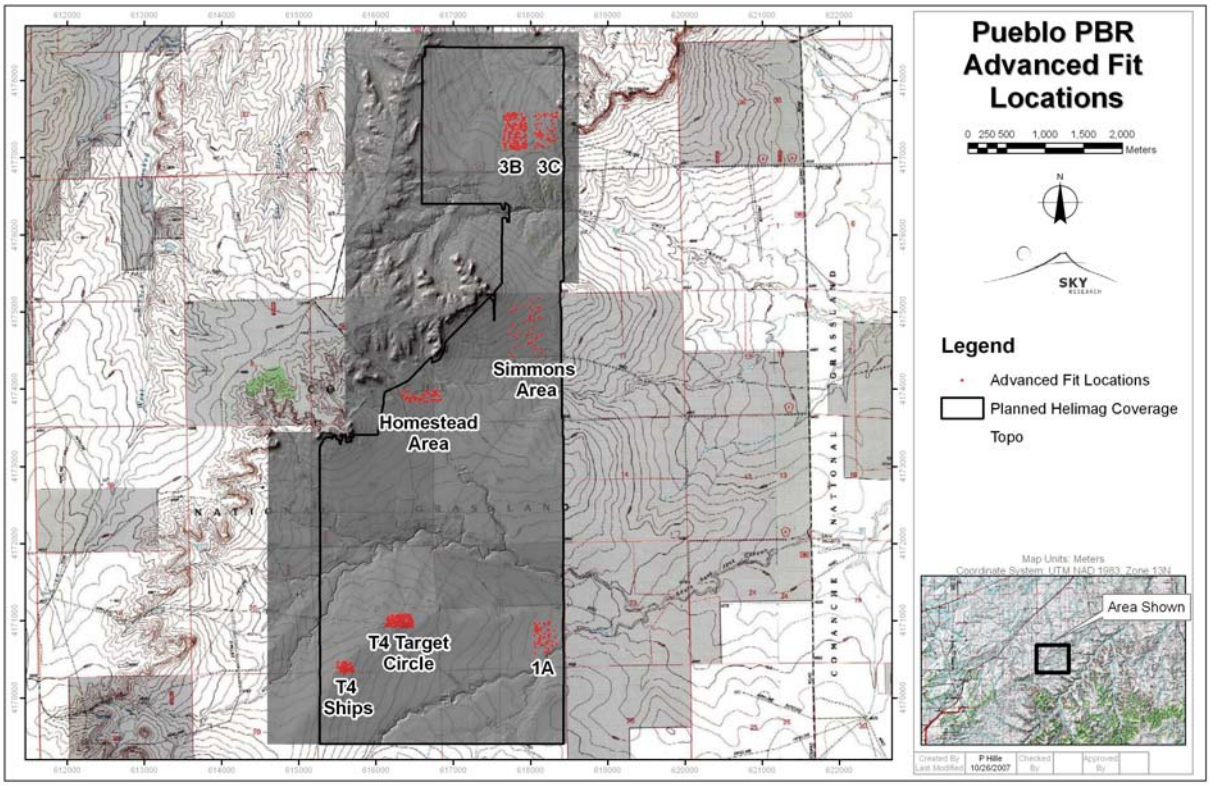

Figure 23. Locations of intrusive investigation areas.

In Figure 24 we present the analysis results with respect to predicted size, depth and dipole angle relative the Earth's magnetic field (i.e. the 'solid' angle). Although the target analysis and subsequent ground truth was not necessarily extensive or comprehensive, there are some interesting patterns to note.

The first pattern we note is the difference between the size and depth distributions for the two 'high density' targets. Most of the predicted depths within the Target Circle area are greater than 0.5 m while the majority of the targets in the Ship area are within 0.5 m of the surface. Similarly the size estimates within the Target Circle area are much larger than those at the Ship area. One explanation for these differences is that the Target Circle area has undergone a clearance

whereby most of the surface or near surface metal has been removed, but larger deep targets still remain. This is also in keeping with the fact that there are no craters within the target circle area itself although it is surrounded by fairly dense cratering (Sky Research 2007).

The 'solid angle' can be used to determine whether a given anomaly has a high level of remanent magnetization. The distortion of the Earth's magnetic field caused by a ferrous object can be due to both induced magnetization and remanent magnetization. Ferrous objects can become demagnetized (i.e., lose their remanent magnetization) through mechanical shock such as the impact undergone by ordnance that has been dropped or fired. The angle of an induced magnetic dipole is constrained to within 60 degrees of the Earth's field. If the solid angle is greater than 60 degrees we attribute that to the presence of a significant remanent magnetic moment and can assume that the object is not related to UXO that has been dropped or fired. Statistically then we assume that for regions contaminated with UXO due to practice bombing the distribution of the solid angles will be heavily skewed towards angles less than 60 degrees.

We would expect this skewing of the solid angle distributions to be the case for the high anomaly density 'Ship' and 'Target Circle' areas and indeed the histograms shown in Figure 24 are in agreement with this expectation. The extreme skewing evident in the Target Circle area may be an artifact of the surface clearance (due differential clean-up of non UXO related material on the surface).

We would also assume that this would not be the case for areas that do not show high anomaly densities. This expectation is based on the assumption that the low density areas are not significantly contaminated with UXO related material. The solid angle distributions for the Simmons Area and Area 1A are more or less evenly distributed from 0 to 180 degrees supporting the assumptions that these areas are not significantly contaminated with UXO related material. However, even though areas 3B and 3C are not associated with high anomaly densities, the solid angle distribution is skewed towards small angles. While this is by no measure conclusive evidence, it does indicate that there is potential for the presence of UXO related material. This conclusion is supported by the dig results (Figure 25) presented in the following section.

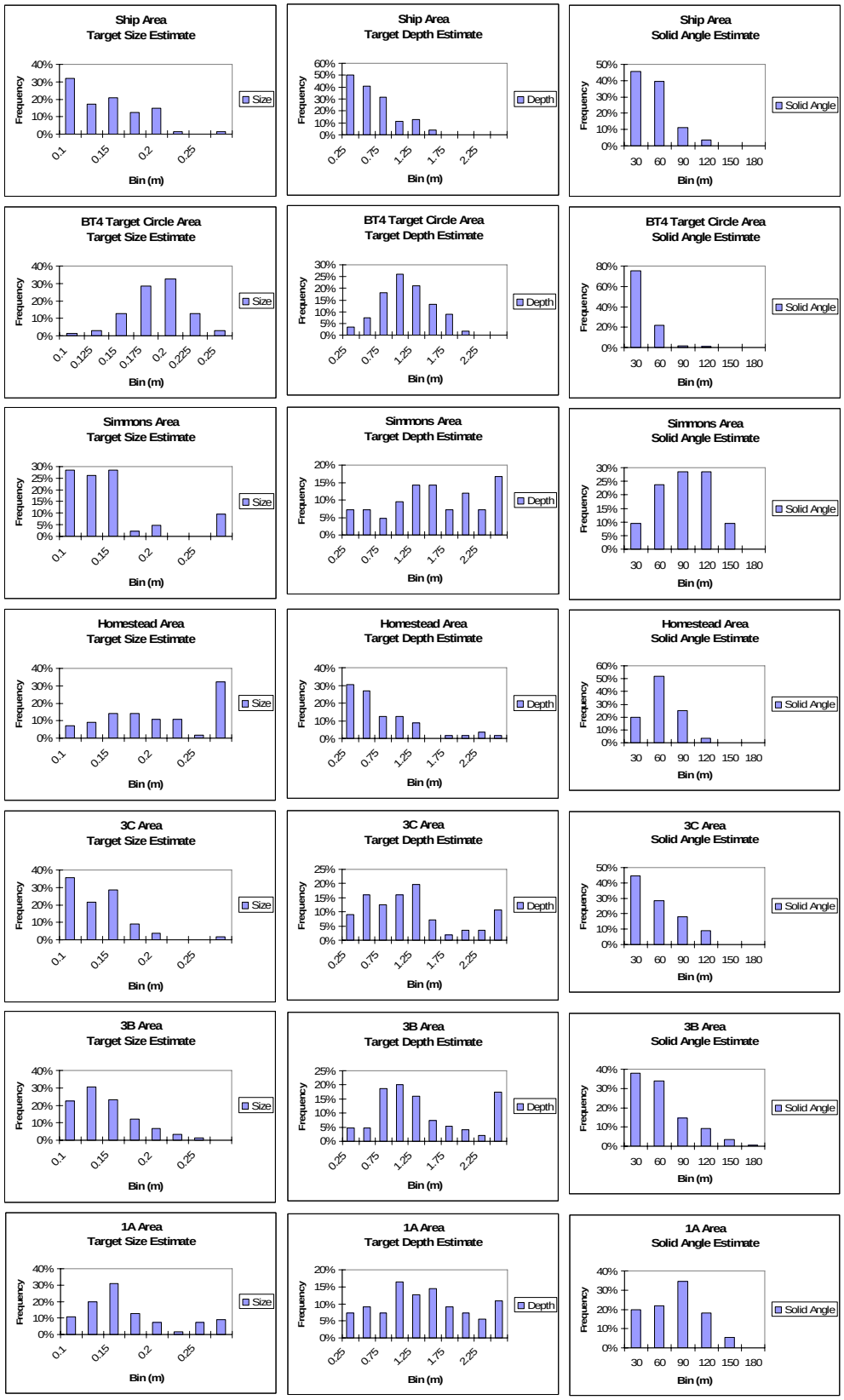

Figure 24. Histograms of dipole fit analysis results. Three Parameters (target size, target depth, solid angle) are presented for each target areas analyzed.

4.2.3. Intrusive Investigation Results

A small number of targets were selected for intrusive investigation to supply ground truth. The dig program included anomalies detected by both the HeliMag system and the vehicular towed system (not a Sky Research endeavor). For each dig, the item was classified as 'Intact UXO', 'UXO related', 'Non-UXO related' or geology ('no-find').The aggregate of dig results are summarized in the charts presented in Figure 25. From these charts we see that there were a relatively large number of 'no-finds' (responses attributed to geology). Upon closer inspection we found that the preponderance of no-finds in the HeliMag results occurred in the Simmons area. This area was not characterized by a high density of anomalies, and the analyst's picks included many 'marginal picks' because we were asked to pick 'into the noise' on this area. Once the Simmons area was excluded from the analysis, the 'no find' rate drops significantly. It is assumed that the vehicular picks will also be skewed towards 'no-find' results for the same reasons.

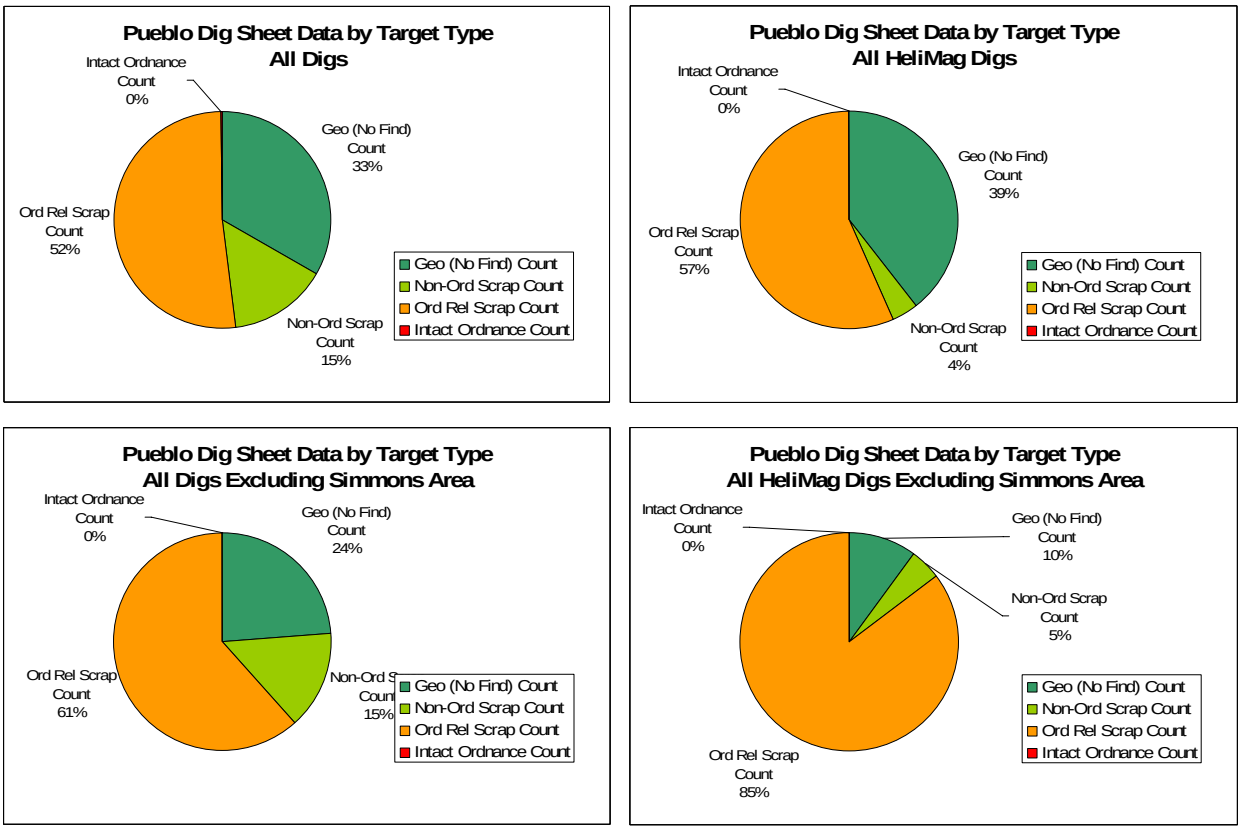

Figure 25. Intrusive investigation results for selected anomalies at the Pueblo Bombing Range.

In Figure 26 we show a breakdown of the intrusive results obtained for the sites listed in Table7. Although there were no advanced analyses performed for anomalies in area Area BT3, we include the dig results in this figure to use as an example of the dig results breakdown in a high anomaly density region. There were no intrusive investigations performed at the Homestead area.

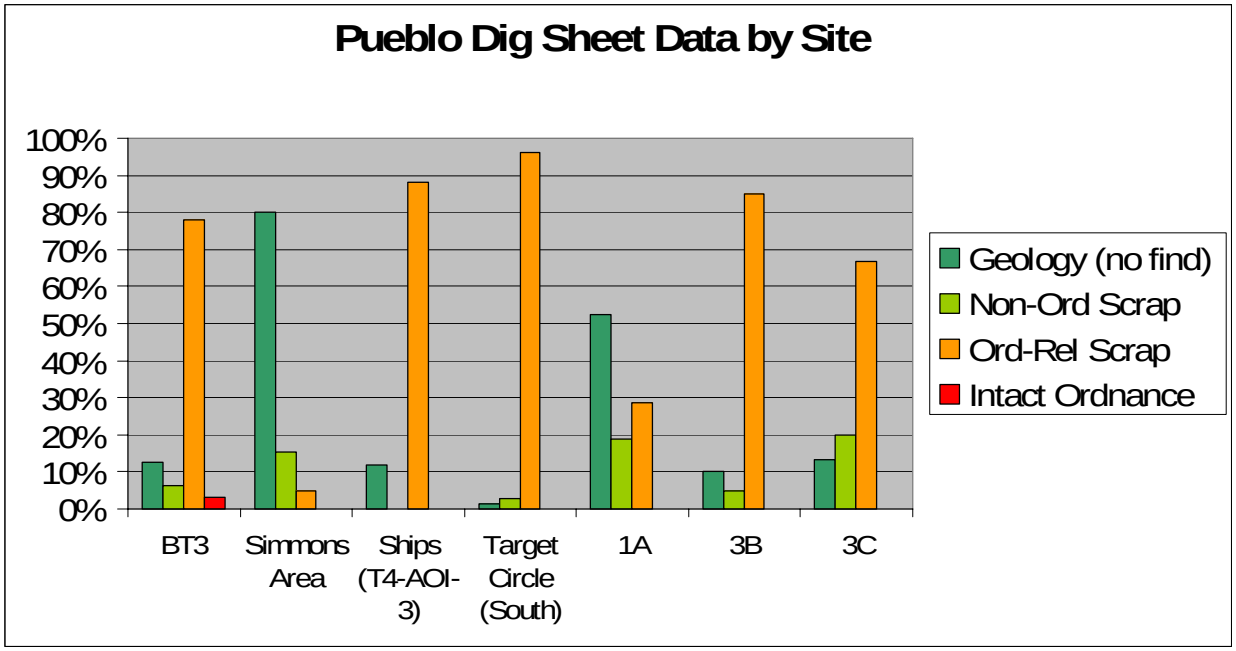

Figure 26. Intrusive investigation results for selected areas at the Pueblo Bombing Range**.**

These intrusive results verify the use of the solid angle distribution as an indicator of potential UXO-related material. Specifically, the Simmons area and (to a lesser extent) area 1A are significantly less contaminated with UXO related material (based upon the % of UXO related finds) than are areas 3B and 3C, even though the overall target density for these four sites is very similar.

4.3. Performance Criteria

The performance of the helicopter magnetometry technology was measured against the criteria listed in Table 8.

Table 8. Performance Criteria for the Pueblo PBR#2 HeliMag Technology Demonstration

Performance Criteria	Description	Type of Performance Objective
Technology Usage	Ease of use and efficiency of operations.	Primary/ Qualitative
Geo-reference position accuracy	Comparison of calibration target dipole fit analysis position estimates (in 3 dimensions) to ground truth	Primary/ Quantitative
HeliMag survey area coverage	Actual # acres surveyed/Planned # of survey acres.	Secondary/ Quantitative
Operating parameters (altitude, speed, production rate)	Valued to be calculated and using average and mean statistical methods to compute each parameter	Secondary/ Quantitative
System Noise	Accumulation of noise from sensors and sensor platforms, including GPS, rotor noise, radio frequencies, etc. calculated as the standard deviation of a 20 sec window of processed data collected out of ground effect.	Primary/ Quantitative
Data density/point spacing.	(# of sensor readings/sec)/ airspeed	Secondary/ Quantitative
MEC parameter estimates	The size and dipole angle estimates of the calibration items are consistent.	Secondary/ Quantitative

4.4. Performance Confirmation Methods

Table 9 details the confirmation methods that were used for each criterion, the expected performance, and the performance achieved.

Position accuracy on a dynamic platform is very difficult to measure precisely. We are able to infer the position accuracy of the sensor data by using the position estimates derived from dipole fit analysis of data collected over known targets. Although there are additional error sources (other than just those due to the data positioning) in the dipole fit results, they are almost negligible due to the stability of the magnetometer calibration and the robustness of the dipole fit process. Because reciprocal passes will tend to hide along-track position errors (due to the robustness of the dipole fit process), the dipole fit analyses were performed on a single pass over the targets. Unfortunately it was determined that some of the validation lane targets had been moved during the survey, so we do not have a precise measure of the position accuracy – from Figures 11 and 12 and historical performance we can estimate that the bias is on the same order

as the standard deviation. So for the purposes of the performance objectives we simply state that the position accuracy was better than 0.25 m. The results for these analyses are presented in Table 9.

The spatial extent of a magnetic anomaly (from our targets of interest) is a factor of two times greater than the sensor offset distance. Based upon our minimum survey height of 1.5 m, we can conservatively define gaps in survey coverage as areas where the distance to the nearest sensor reading is greater than 2 m. Gaps in survey coverage are generally related to navigation (a combination of pilot skill, topography/vegetation, and wind conditions) or data integrity (primarily GPS fix quality). As a general practice, images representing the data from each day of survey flying are created to identify areas requiring fill-in flying to cover significant gaps in coverage. Invariably there will be a number of gaps in survey coverage that cannot be practically filled. To estimate the survey coverage performance, at every 0.25 m interval (grid node) we search through a 1 m radius for a valid data point. The number of grid nodes where valid data are found is divided by the total number of grid nodes to derive the percentage of survey coverage. Based upon these factors and acreages, the final coverage was 99.29%.

The assessment of the survey altitude and speed was performed by extracting statistics for these parameters from the survey databases. Survey speed was consistently maintained between 20 and 45 knots, with some insignificant variation at the beginning or end of the survey lines. Survey altitude is a critical parameter for this type of investigation and is expected to be a little more variable than survey speed. In Figure 27, we present a histogram of the survey altitude performance. As with presentation/analysis of the results, prior to deriving these statistics, all altitudes above 3 m were rejected. These altitudes generally occur at the end of survey lines or during times when the helicopter has broken off a survey line and is circling back to reacquire it. The mean survey altitude was 1.4 m and the standard deviation was 0.42 m.

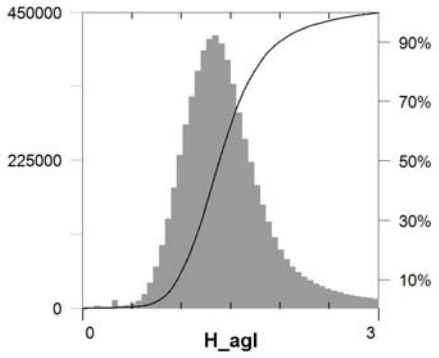

Figure 27. Histogram of sensor altitude above ground level.

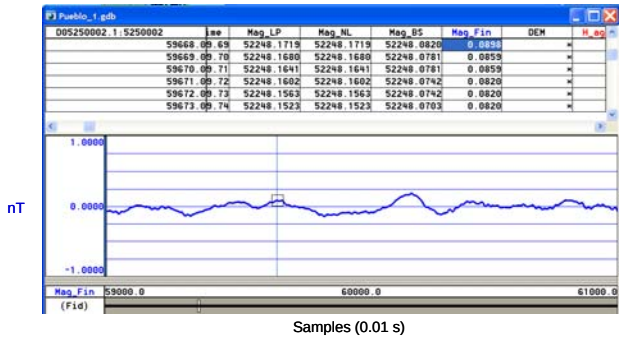

HeliMag system noise levels were determined by calculating the standard deviation of the final filtered magnetic data flown at high altitude out of ground effect. The noise varied by sensor/orientation with the Earth's field. Typical results varied from 0.07 to 0.11 nT. Figure 28 depicts a typical 20 s stretch of high altitude data.

Figure 28. Filtered, 'final' magnetometer data taken at high altitude.

The cross-track data density is essentially static and is a function of the system geometry. With the exception of isolated data gaps (addressed above) the 'worst case' spacing is our sensor spacing of 1.5 m. The effective density is much higher than this due to the significant overlap required to ensure (or at least minimize) data gaps due to the inevitable cross-track variation of the helicopter flight path. However, because the density is not uniform, we quote the 'worst case' as the data density achieved. Down-track data density is much higher than the cross-track density and is a function of survey speed. At our final sample rate of 100 Hz, the survey speeds of 11 – 23 m/s (21 – 45 knots) resulted in down-line data spacing of 0.11 - 0.23 m.

Table 9. Performance Metrics Confirmation Methods and Results

Performance Metric	Confirmation Method	Expected Performance	Performance Achieved
Technology Usage	Field experience using technology during demonstration	Relative ease of use	Pass
Geo-reference position accuracy	Infer sensor position accuracy from position estimates of calibration targets derived using dipole analysis of repeated data collection over calibration targets	Horizontal < 0.25 m Vertical <0.5 m	Horizontal: Mean 0.25 m (SD 0.18 m) Vertical: Mean 0.39 m (SD 0.19 m)
HeliMag survey area coverage	The sum of actual areas surveyed will be calculated in geographic information system (GIS) and compared to the 5,056 acres planned for survey.	95%	99.29%
Operating parameters (altitude, speed, overlap, production level)	Field data logs will be used to calculate the operating parameters	Altitude: 1-3 m AGL Speed: 15-20 m/s (30-40 knots) Production 300 acres/day	Altitude: Mean 1.44m SD 0.42 m Speed: Mean 17.4m/s SD 3.0 m/s Production:456 acres/day
System Noise	The system noise will be calculated as the standard deviation of a 20 s window of processed high-altitude data.	<1 nT	0.11 nT
Data density/point spacing.	Calculated based upon system sample rate and survey speed (along track) and system geometry and survey line spacing (cross track).	0.5 m along-track 1.5 m cross track	Along-track: Mean 0.17 m Cross-track: 1.5 m (Max)
MEC parameter estimates	Comparison of analysis results of repeated data collected over calibration targets.	Size <0.02 m Solid Angle < 10º	Size: SD 0.011 m Solid Angle 7º

5. COST ASSESSMENT

5.1. Cost Reporting

Cost information associated with the demonstration of all airborne technology, as well as associated activities, was tracked and documented before, during, and after the demonstration to provide a basis for determining the operational costs associated with this technology. For this demonstration, Table 10 contains the cost elements that were tracked and documented for this demonstration. These costs include both operational and capital costs associated with system design and construction; salary and travel costs for support staff; subcontract costs associated with airborne services, support personnel, and leased equipment; and costs associated with the processing, analysis, comparison, and interpretation of airborne results generated by this demonstration. The magnetometers used for the HeliMag technology were provided through a CRADA with NRL; as such, the actual cost of using the technology was not captured in this demonstration. However, we will estimate the true cost of using this technology, in addition to the cost and performance of all technologies demonstrated, in the ESTCP Cost and Performance Report to be submitted following this demonstration.

5.2. Cost Analysis

The single largest cost element for an airborne survey is the cost of aircraft airtime. In addition, mobilization costs for the helicopter can be significant. Generally, mobilization cost is a function of distance from the home base for the aircraft, equipment, and personnel. Because the helicopter was mobilized a relatively short distance (from Denver to La Junta) the costs for mobilization and demobilization for this demonstration were significantly less than would have been encountered for a demonstration site further away. Data processing and analysis functions made up the bulk of the remaining costs.

Project management and reporting were a significant cost for this demonstration, as the project was conducted under the WAA pilot program and required more meetings, travel, and reporting than would generally be expected for a production level survey.

Costs associated with validation were not considered in the cost analysis, as the validation was conducted as part of the WAA pilot program.

Table 10. Cost Tracking

COST CATEGORY	SUB CATEGORY	DETAILS	COSTS ($)
START-UP COSTS	Pre-Deployment and Planning	Includes planning, contracting, site visit, and site inspection	$36,864
	Mobilization	Personnel mobilization, equipment mobilization, and transportation	$15,444
OPERATING COSTS	Helicopter Survey	Data acquisition and associated tasks, including 70.4 hours of helicopter operation time and 10.8 hours of standby time	$144,221
DEMOBILIZATION	Demobilization	Demobilization, packing, calibration line removal	$14,840
DATA PROCESSING AND ANALYSIS	Data Processing	Initial and secondary processing of data	$19,126
	Data Analysis	Analysis of airborne magnetometry datasets	$80,525
MANAGEMENT	Management and Reporting	Project related management, reporting and contracting	$77,121
TOTAL COSTS			
		Total Technology Cost	$388,141.00
		Acres Characterized	5,020
		Unit Cost	$77.32/acre

6. IMPLEMENTATION ISSUES

6.1. Regulatory and End-User Issues

The ESTCP Program Office established a Wide Area Assessment Pilot Program Advisory Group to facilitate interactions with the regulatory community and potential end-users of this technology. Members of the Advisory Group include representatives of the U.S. Environmental Protection Agency, State regulators, U.S. Army Corps of Engineers officials, and representatives from DoD. ESTCP staff have worked with the Advisory Group to define goals for the Pilot Program and develop Project Quality Objectives. As the analyzed data from the demonstrations has become available, the Advisory Group assisted in developing a validation plan.

There are a number of issues to be overcome to allow implementation of WAA beyond the pilot program. Most central is the change in mindset that will be required if the goals of WAA extend from delineating target areas to collecting data that is useful in making decisions about areas where there is not indication of munitions use. A main challenge of the pilot program is to collect sufficient data and perform sufficient evaluation that the applicability and limitations of these technologies in delineating uncontaminated land are well understood and documented. Similarly, demonstrating that WAA data can be used to provide information on target areas regarding boundaries, density and types of munitions to be used for prioritization, cost estimation, and planning will require that the error and uncertainties in these parameters are well documented in the program.

7. REFERENCES

Blakely, R.J. and R. W. Simpson, 1986, "Approximating edges of source bodies from magnetic or gravity anomalies," *Geophysics*, v.51, p.1494-1498.

Nelson, H., J. McDonald and D. Wright, April 2005, "Airborne UXO Surveys Using the MTADS," Naval Research Laboratory NRL/MR/6110--05-8874.

Office of the Under Secretary of Defense for Acquisition, Technology, and Logistics, December 2003, "Report of the Defense Science Board Task Force on Unexploded Ordnance," 20301-3140.

Sky Research, October 2007, "Draft Final Wide Area Assessment Demonstration of LiDAR and Orthophotography at Pueblo Precision Bombing Range".

Tuley, M. and E. Dieguez, July 2005, "Analysis of Airborne Magnetometer Data from Tests at Isleta Pueblo, New Mexico," IDA Document D-3035.

United States Army Corps of Engineers, St. Louis District, 1995, Archive Search Report.

Versar, 2005, "Former Kirtland Precision Bombing Range, Conceptual Site Model, V0".

8. POINTS OF CONTACT

Table 11. Points of Contact

POINT OF CONTACT	ORGANIZATION NAME ADDRESS	CONTACT INFORMATION	ROLE
Dr. John Foley	Sky Research, Inc. 445 Dead Indian Road Ashland, OR 97520	(Tel) 978.479.9519 (Fax) 720.293.9666	Principal Investigator
Mr. David Wright	Sky Research, Inc. 445 Dead Indian Road Ashland, OR 97520	(Tel) 919.303.3532	Co-Principal Investigator
Mr. Jerry Hodgson	USACE Omaha District 215 N. 17th Street Omaha, NE 68102-4978	(Tel) 402.221.7709 (Fax) 402.221.7838	Federal Advocate
Mr. Hollis (Jay) Bennett	US Army R&D Center (CEERD-EE-C) 3909 Halls Ferry Road Vicksburg, MS 39180-6199	(Tel) 601.634.3924	DoD Service Liaison

Project Lead Signature: